Novel sediment sampling method provides new insights into vertical grain size variability due to marine and aeolian beach processes

van IJzendoorn, Christa O.; Hallin, Caroline; Cohn, Nicholas; Reniers, Ad J.H.M.; De Vries, Sierd

DOI
10.1002/esp.5518

Publication date
2022

Document Version
Final published version

Published in
Earth Surface Processes and Landforms

Citation (APA)
van IJzendoorn, C. O., Hallin, C., Cohn, N., Reniers, A. J. H. M., & De Vries, S. (2022). Novel sediment sampling method provides new insights into vertical grain size variability due to marine and aeolian beach processes. *Earth Surface Processes and Landforms*, *48*(4), 782-800. https://doi.org/10.1002/esp.5518

Received: 13 May 2022 | Revised: 14 November 2022 | Accepted: 17 November 2022

DOI: 10.1002/esp.5518

RESEARCH ARTICLE

ESPL WILEY

Novel sediment sampling method provides new insights into vertical grain size variability due to marine and aeolian beach processes

Christa O. van IJzendoorn[1] | Caroline Hallin[1,2] | Nicholas Cohn[3] | Ad J. H. M. Reniers[1] | Sierd De Vries[1]

[1]Faculty of Civil Engineering and Geosciences, Delft University of Technology, Delft, The Netherlands

[2]Division of Water Resources Engineering, Faculty of Engineering, Lund University, Lund, Sweden

[3]Coastal and Hydraulics Laboratory, US Army Engineer Research and Development Center, Duck, North Carolina, USA

Correspondence
Christa O. van IJzendoorn, Faculty of Civil Engineering and Geosciences, Delft University of Technology, Stevinweg 1, 2628 CN. Delft, The Netherlands.
Email: c.o.vanijzendoorn@tudelft.nl

Funding information
Dutch Research Council (NWO), Grant/Award Number: 17064; Engineer Research and Development Center, Grant/Award Number: Program Element 601102/Project AB2/Task 01

Abstract

In sandy beach systems, the aeolian sediment transport can be governed by the vertical structure of the sediment layers at the bed surface. Here, data collected with a newly developed sand scraper is presented to determine high-resolution vertical grain size variability and how it is affected by marine and aeolian processes. Sediment samples at up to 2 mm vertical resolution down to 50 mm depth were collected at three beaches: Waldport (Oregon, USA), Noordwijk (the Netherlands) and Duck (North Carolina, USA). The results revealed that the grain size in individual layers can differ considerably from the median grain size of the total sample. The most distinct temporal variability occurred due to marine processes that resulted in significant morphological changes in the intertidal zone. The marine processes during high water resulted both in fining and coarsening of the surface sediment. Especially near the upper limit of wave runup, the formation of a veneer of coarse sediment was observed. Although the expected coarsening of the near-surface grain size during aeolian transport events was observed at times, the opposite trend also occurred. The latter could be explained by the formation and propagation of aeolian bedforms within the intertidal zone locally resulting in sediment fining at the bed surface. The presented data lays the basis for future sediment sampling strategies and sediment transport models that investigate the feedbacks between marine and aeolian transport, and the vertical variability of the grain size distribution.

KEYWORDS
aeolian, coastal geomorphology, coastal processes, grain size, intertidal beach, sediment availability, sediment transport

1 | INTRODUCTION

Aeolian sediment transport rates and threshold velocities depend on the grain size composition of the bed (Bagnold, 1937b). Meanwhile, aeolian transport alters the composition of the bed surface through grain size-selective pickup and deposition (Bagnold, 1937a; Bauer, 1991), and underlying sediment layers may be exposed through erosion. When underlying sediment is exposed, aeolian transport rates depend not only on the grain size composition of the uppermost surface layer (< 2 mm) but on the vertical variability in grain size distribution of the bed. In the intertidal zone, the grain size composition is influenced by both aeolian and marine processes (Figure 1) as wave and tide induced currents erode and deposit sediment and rework the bed (Reniers et al., 2013; Srisuwan & Work, 2015). Since the intertidal zone can be an important sediment source for aeolian transport (de Vries et al., 2014), the resulting grain size composition and vertical stratigraphy could impact total transport rates from the beach towards the dunes. This study analyses the temporal and spatial grain size variability of millimeter-thick vertical layers of the intertidal bed using a new sediment sampling device.

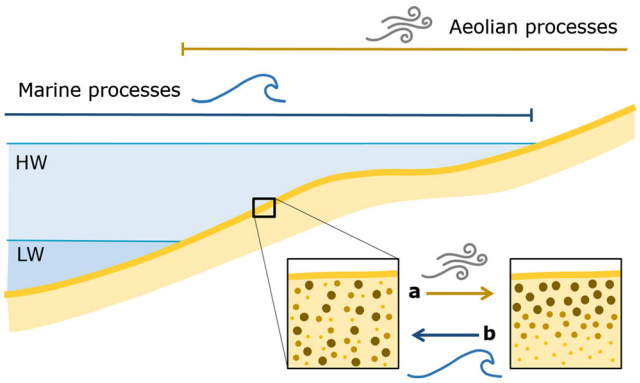

FIGURE 1 Marine and aeolian processes overlap in the intertidal zone between the most seaward location that becomes exposed and the most landward location that becomes inundated. Note that these boundaries vary in time and space depending on beach morphology, tides, waves and runup. When considering the vertical variability of the grain size distribution, marine and aeolian processes could, for example, have the following effects: (a) aeolian transport may cause coarsening of the upper layer of the surface due to selective pickup by the wind during low tide; (b) marine processes may cause homogenization of the vertical grain size layering due to mixing occurring during high tide, which results in an increase of fine particles near the surface. It should be noted that the schematized effects of the marine and aeolian processes in this figure are only examples, and that other effects also can occur.

During aeolian sediment transport, the grain size distribution at the sediment surface can change as the wind selectively picks up grains from the surface. Wind-blown sand deposits are generally dominated by sediments with a grain size between 150 and 300 μm, with some grains as fine as 80 μm (Bagnold, 1941). The sediment in the source areas is typically less well-sorted with larger fractions of coarser elements (Bagnold, 1937a; Bauer, 1991). At the bed surface where the wind-blown sediment originates, an increase in the grain size can be expected when the finer grains are removed. This increase in grain size was observed by Field and Pelletier (2018) in an arid dune field. On a beach in Duck, North Carolina, USA, Cohn et al. (2022) similarly observed a gradual coarsening within the saltation layer at a sub-hourly timescale despite decreasing wind speeds, which may indicate an increase in grain size at the bed surface. Coarsening of the bed can result in armoring effects that reduce the aeolian transport rates because the coarse particles cannot be moved by the wind. For example, Strypsteen et al. (2021) observed that a coarse armor layer on Texel, the Netherlands, was immobile for wind speeds up to 15 m/s.

The potential for sediment transport by marine processes is expected to be larger, as marine processes are typically a more powerful driver of sediment transport than aeolian processes (e.g., de Vries et al., 2014; Hoonhout & de Vries, 2017; Van der Wal, 2000). Marine processes that can affect the grain size layering in the intertidal area are, for instance, sediment overturning and mixing by waves, (tidal) currents, swash and backwash (e.g., Jackson & Nordstrom, 1993; Masselink & Puleo, 2006). Generally, it is thought that the depth of mixing is larger in the lower parts of the intertidal zone, coincident with larger wave dissipation (Anfuso, 2005; Jackson & Nordstrom, 1993; Sherman et al., 1993; Voulgaris & Collins, 2000). Apart from sediment mixing, the removal and supply of sediment through advection can affect spatio-temporal grain size variations (Aagaard & Greenwood, 2008; Jackson et al., 2004; Osborne & Rooker, 1999). Erosion can expose sediment layers with distinctly different grain sizes (Gallagher et al., 2016). Bedform (e.g., bar, berm, rip channels) migration can cause mixing (Sherman et al., 1993). Additionally, cross-shore variations in grain size are caused by these morphological features so they can cause changes in grain size when they migrate (e.g., Gallagher et al., 2011; Medina et al., 1994; Sonu, 1972; Van der Zanden et al., 2017).

The multitude and complexity of marine processes in the intertidal zone make it difficult to predict the resulting grain size distribution and stratigraphy after inundation due to, for example, high tide, storm surge, wave setup, and swash. Several field studies have shown a cross-shore gradient in grain size across the intertidal zone (Bauer, 1991; Çelikoğlu et al., 2006; Edwards, 2001; Sonu, 1972; Stauble & Cialone, 1997). Additionally, several model studies have shown that marine processes may result in a vertical variability in the grain size distribution (Reniers et al., 2013; Srisuwan & Work, 2015). Gallagher et al. (2016) observed this type of variability on the decimeter- to meter-scale in the field. However, from the perspective of aeolian transport, vertical scales of millimeter up to centimeter are of interest. Field data on the vertical grain size variability at the sub-centimeter scale within the intertidal zone could provide insight into the influence of the interplay between marine and aeolian processes on the bed composition and sediment supply for aeolian transport.

Several methods and sampling techniques are available for grain size analysis in coastal environments. Surface photographs (Barnard et al., 2007; Buscombe et al., 2010; Rubin, 2004) can be used to study the top of the bed surface. Trenching (Gallagher et al., 2016), sand peels (Yasso & Hartman, 1972; Yokokawa & Masuda, 1991), and sediment coring (Gallagher et al., 2016; Gunaratna et al., 2019) can be used to study larger scale (vertical) patterns in grain size. Another method is surface grab sampling (or bulk sampling), in which typically the top 5–10 cm of the bed surface is collected (Gallagher et al., 2011; Hallin et al., 2019; Huisman et al., 2016; Masselink et al., 2007; Medina et al., 1994; Prodger et al., 2017; Reniers et al., 2013; Stauble & Cialone, 1997). Combinations of these methods are possible, for instance, as shown by Gallagher et al., 2016, who used sediment coring, a digital imaging system (similar to surface photographs) and trenching. However, none of these methods have shown to facilitate feasible sub-centimeter detailed sampling of the vertical grain size variability in the intertidal zone.

In this study, a new sand scraper method is introduced that allows for measurements of vertical variability of grain size distribution with a resolution of 2 mm down to 50 mm depth. The sand scraper is used to collect samples from three different beaches in Waldport (Oregon, USA), Noordwijk (the Netherlands) and Duck (North Carolina, USA). For these three case studies, it is investigated (1) whether near-surface sediment layers differ in grain size from the median grain size derived from bulk sampling, (2) the effect of aeolian sediment transport on vertical grain size layering, and (3) the effect of marine processes on vertical grain size layering at the intratidal timescale.

This article presents the methodology and sampling strategy used to obtain the vertical variability of the grain size distribution (Section 2). Additionally, the collected data per field site are shown, including samples that were collected to provide insight into the repeatability of the sampling method, the presence of bedforms and the occurrence of spatial variability (Section 3). Following, the spatio-temporal trends in grain size due to both marine and aeolian processes, the advantages and disadvantages of the sand scraper sampling method, and the implications for sediment availability and future research are discussed (Section 4).

2 | METHODOLOGY

2.1 | Field sites

This study was conducted by collecting sediment samples showing the vertical variability of the grain size distribution in Waldport (Oregon, USA), Noordwijk (the Netherlands) and Duck (North Carolina, USA) (Figure 2). The three beaches have different hydrodynamic and morphological characteristics (Table 1). Beach widths above mean sea level range from less than 50 m in Duck to 200 m in Waldport.

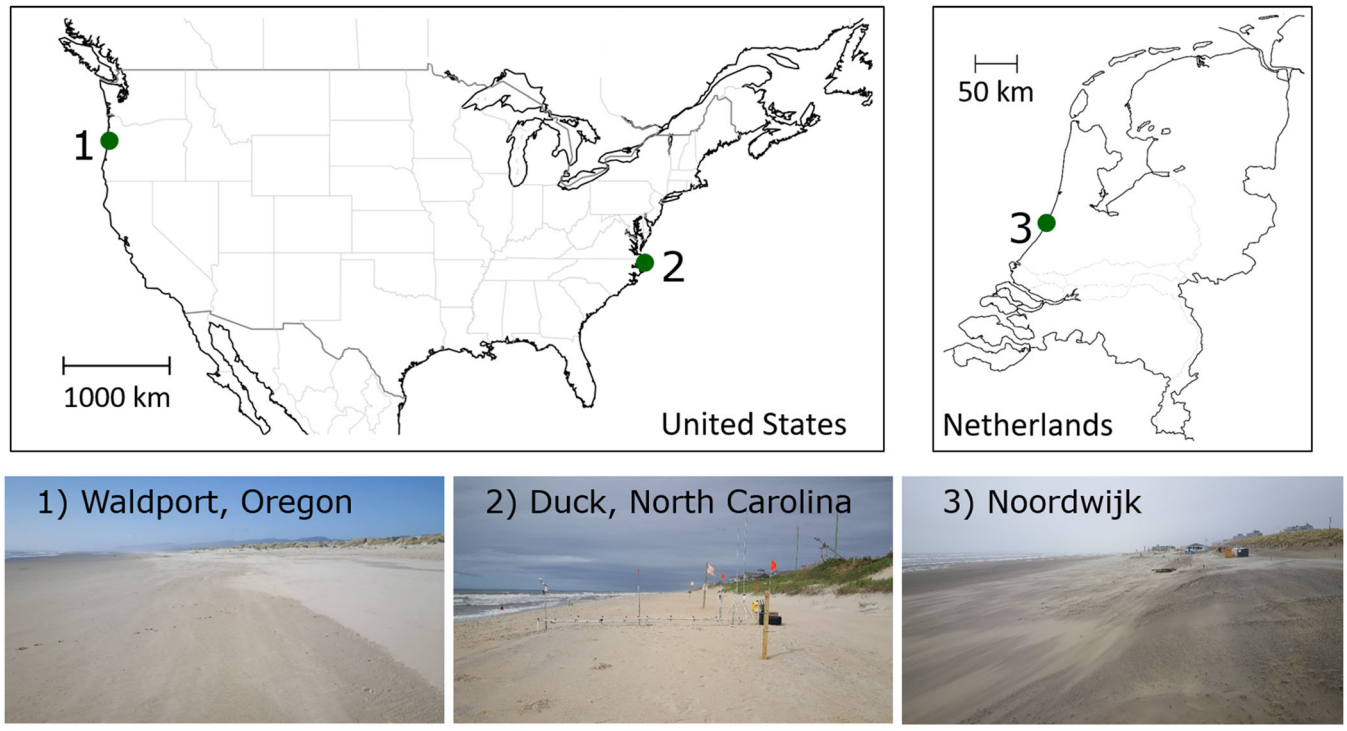

FIGURE 2 Locations where vertical grain size distributions were collected in the United States (Waldport, Oregon and Duck, North Carolina) and the Netherlands (Noordwijk). The numbers in the maps correspond to those of the photographs. Pictures 1 and 2 were mirrored horizontally to aid comparison between locations. Photographs: Christa van IJzendoorn

TABLE 1 Overview of morphological and marine characteristics of field sites in Waldport (Oregon, USA), Noordwijk (the Netherlands) and Duck (North Carolina, USA)

	Waldport	Noordwijk	Duck
Sampling location	N 44°26′13.5″, W 124°5′5.1″	N 52°14′31.9″, E 4°25′29.5″	N 36°11′5.2″, W 75°45′6.3″
Beach slope	1:40[a]	1:30	1:15[g]
Beach width (m)	200[a]	100–150	<50
Tidal range (m)	1.5–2[b]	1.4[e]	1.0
Springtide range (m)	3–4[b]	1.8[e]	1.5
Mean wave height (m)	1.5[c] (summer)	1	1
Storm wave height (m)	10[b]	5	6[h]
Expected grain size (D_{50}) (μm)	200–250[d]	250–300[f]	300 (with coarser present)[i]

[a]Based on beach data available through http://nvs.nanoos.org/.
[b]Ruggiero et al., 2010.
[c]Tillotson & Komar, 1997.
[d]Twenhofel, 1946.
[e]Ojeda et al., 2008.
[f]van Bemmelen, 1988.
[g]Doran et al., 2015.
[h]Larson & Kraus, 1994.
[i]Gallagher et al., 2016.

Compared to the other beaches, Waldport has a larger spring tide range and the highest storm waves. The beach in Duck is distinct from the others because it is intermediate (compared to dissipative), micro-tidal, and mixed grained. Additionally, the lower beach morphology in Noordwijk and Waldport are dominated by the presence of intertidal bars, while the beach in Duck has a pronounced berm. The expected median grain size for the different sites ranges from 200 to 250 μm in Waldport to > 300 μm in Duck.

2.2 | Sediment sample collection and analysis

A new instrument has been developed to measure the vertical grain size variability at the appropriate scales of interest to sediment availability for aeolian sediment transport (Figure 3). The custom-made sand scraper was inspired by a surface sediment sampler presented by Wiggs et al. (2004). The sand scraper consists of a base plate (59 cm × 40 cm) and a sand scraper mechanism (32 cm × 16 cm × 28 cm, Figure 3a). The base plate can be placed on the beach surface and the sand scraper mechanism is then inserted through the base plate into the sand. A dialing mechanism with depth bars that is attached to the base plate determines how deep the sand scraper mechanism is inserted into the sand (Figure 3a). The sediment can be scraped off from the beach surface in precise layers of 2 mm down to 50 mm depth (Figure 3b).

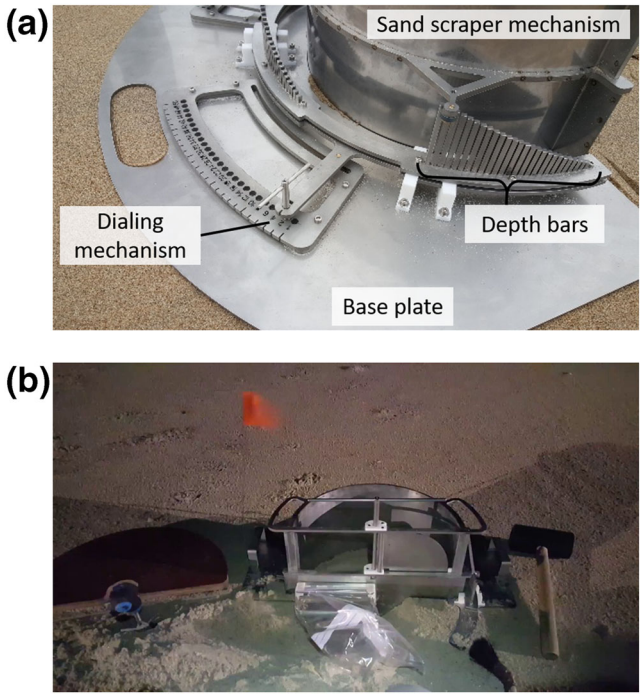

FIGURE 3 Overview of sampling with the sand scraper. (a) The dialing mechanism on the base plate that is used to set the depth at which a sample is collected with the sand scraper mechanism. (b) The sand scraper in use on the beach, surrounded by the top plate, sampling bags, a brush and a small shovel that are used to collect the sand samples. This photograph is a still of a video that is published in the 4TU repository as video 1.mp4 (10.4121/c.5736047). The video shows how one layer can be collected in a sample bag. Subsequently, the dialing mechanism can be used to increase the sampling depth, then, the sand scraper mechanism can be pressed deeper into the sand and the layer collection can be repeated with a new sampling bag.

The base plate and sand scraper mechanism were constructed out of sheets of stainless steel, and they can fit into a shipping box of 60 cm × 40 cm × 40 cm when disassembled. Together, these elements weigh a total of 8.5 kg. Thus, one person can handle the device but for extended walking distances the use of a hand cart for transportation is recommended. The main costs of device construction for this research were labor costs associated with the design and testing of the device. The costs of reproduction will depend on hourly labor costs and the production facilities available. In case of a well-equipped workshop with a water jet cutter and spot-welding capabilities at its disposal, production time and cost might be limited to one work week. More information on the design of the sand scraper is available in the 4TU repository (10.4121/c.5736047).

The scraper was designed for sampling of flat beds within the intertidal area. The device can be used on irregular surfaces but the layered sampling will then be less accurate, especially at the top layer. The maximum sampling depth of 50 mm was chosen to reflect the upper portion of the bed that determines sediment supply for aeolian transport. Thus, it is not expected that the device can fully measure mixing effects that occur due to marine processes as these often have a sediment disturbance that is deeper than 50 mm (Anfuso, 2005; Voulgaris & Collins, 2000). The 2 mm vertical increment was chosen to be only a (few) grain diameter(s) thick to assess micro-scale changes not achievable with conventional grab sampling.

The scraper has a 16 cm radius (0.04 m^2 surface) so that a 2 mm sampling layer, results in a big enough sample for sieving, that is, approximately 150 g. Depending on the required application needs, multiple 2 mm samples can be combined into one bigger sample to reduce the layering resolution. For this research, a more detailed layering resolution was chosen near the surface (i.e., layers of 2 and 4 mm) compared to deeper in the bed (i.e., layers of 6 mm). In total, 10 samples per sampling location were collected when sampling down to 50 mm depth. The sample collection with the sand scraper requires removal of sediment. Therefore, when following the development of the bed through time, consecutive measurements at the same sampling location need to be completed at an adjacent location (< 3 m).

The samples collected with the sand scraper were oven-dried and then analyzed to determine their grain size distribution (Figure 4). The grain sizes of the samples from Noordwijk were determined by dry sieving with 10 sieve screens ranging from 63 μm to 3350 μm, based on BS1377-2 (1990). The grain sizes of the samples from Waldport and Duck were determined using a Camsizer (Retsch Technology, Haan, Germany). The grain size range of the Camsizer was set between 20 and 2000 μm and divided into 200 bins.

From the obtained grain size distributions, various grain size characteristics were determined. First, the median grain size, D_{50} was determined per layer as an indication of the primary grain size characteristics at each site, location and depth. Second, the D_{16}, D_{25}, D_{75}, and D_{84} quantiles were calculated to assess the width of the distribution and the corresponding contributions of the finer and coarser particles within each sample. Third, the weighted average median grain size of all layers in a cross-section, $ø_{50}$, was calculated. This value can be seen as a representation of the D_{50} that would have been found if a bulk sample was collected.

The results are presented in color-coded boxplots. Figure 5 illustrates three example results based on synthetic data as a guide to interpreting the results. Figure 5(a) shows an example where the grain size is larger near the surface (2 mm bin) than the grain size sampled at larger depths (e.g., 50 mm depth). When there is a gradual change in grain size between this relatively coarse surface sample and relatively fine deeper sample, this is henceforth referred to as a fining downward gradient. Conversely, the opposite trend in which there is a gradual increase in grain size from the surface to deeper depths, such as shown in Figure 5(b), is referred to as a coarsening downward gradient. Not all trends shown in the data are gradual. Boundaries, where there are large jumps in grain size, are also noted, as shown in the example in Figure 5(c) at 20 mm depth. The examples provided in Figure 5 also show how increased vertical resolution could aid in studying the sediment availability at the bed surface. For instance, Figure 5(b,c) have a similar $ø_{50}$ but in Figure 5(b) fine sediment is available at the surface, whereas coarse sediment is present at the surface in Figure 5(c) which impedes aeolian sediment transport.

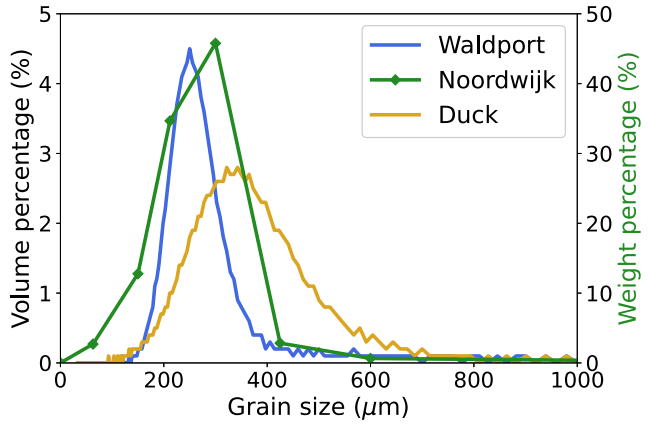

FIGURE 4 Representative grain size distributions for the three different field sites (Waldport, Noordwijk, and Duck). The Waldport and Duck graphs were determined based on 200 grain size bins for which the volume weighted percentage was determined by a Camsizer. The Noordwijk graph was based on sieve analysis, so the weight percentage per sieve size (indicated by the green diamonds) is shown on the right *y*-axis. When assuming that the particle density is constant, the particle size distribution based on volume and mass are the same, allowing for comparison between the different graphs.

2.3 | Sampling strategy

The influence of marine processes and aeolian transport on the vertical grain size variability was studied by repeating the sand scraper sampling at specific times during the tidal cycle (Figure 6). To study the effect of marine processes on the observed grain sizes, samples were collected right before high water (B-HW) and after high water (A-HW), thus, excluding contributions from aeolian transport. To study the bed surface after aeolian transport, samples were collected right after high water and right before high water (after aeolian transport [A-AT]), thereby excluding marine processes. Preferably, measurements were executed during consecutive low and high waters to link the effects of the marine and the aeolian processes. However, in some instances, the environmental conditions only allowed sample collection around a single high water or a single aeolian transport event. In most cases, the limiting factor was the occurrence of aeolian transport during low water.

Several studies have shown that beaches show a cross-shore gradient in grain size (e.g., Çelikoğlu et al., 2006; Stauble & Cialone, 1997), and spatial variations in aeolian transport can occur in the intertidal area related to spatial patterns in moisture content (e.g., Davidson-Arnott et al., 2008) and the fetch effect (e.g., Delgado-Fernandez, 2010). To take these spatial variations into account, three locations throughout the intertidal zone were sampled during each field experiment.

The exact sampling locations in the intertidal zone were determined by the extent of the swash/tide excursion during the high water and extent of the area affected by aeolian transport. The most seaward sampling location should not be too close to the low water line as there is no transport expected due to the high moisture content and, with onshore directed wind, due to the fetch effect.

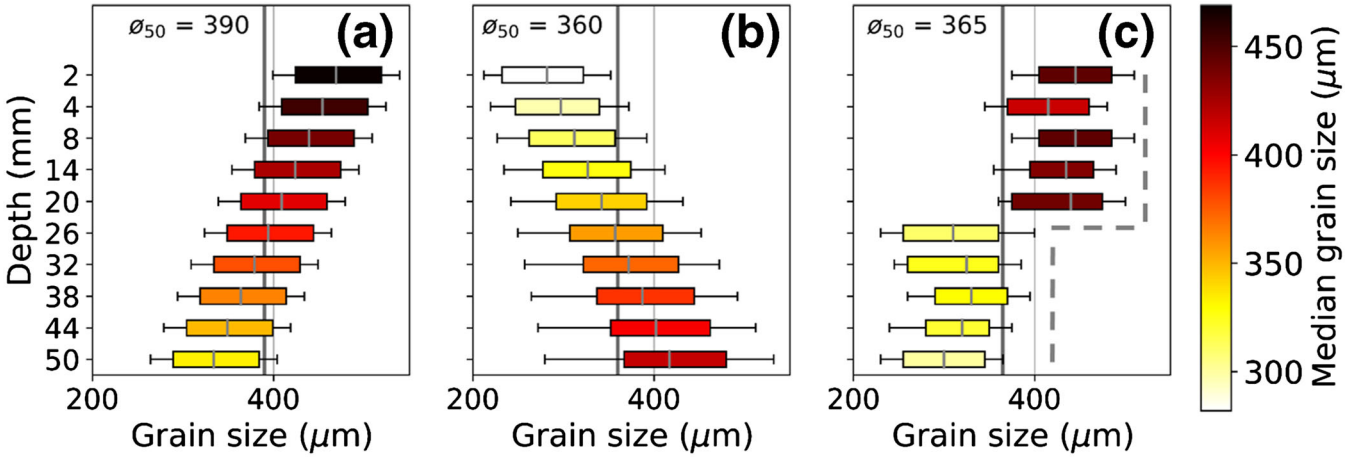

FIGURE 5 Synthetic data used to show examples of vertical variability in the grain size distribution. Colors indicate the median grain size. Box plot dimensions are based on the D_{25} and D_{75}, and the extent of the whiskers on the D_{16} and D_{84}. For each vertical grain size distribution, the $ø_{50}$ is included. (a) A fining downward gradient, (b) a coarsening downward gradient with widening distribution with depth and (c) coarser sediment on top of finer sediment, with a boundary at 20 mm depth, which is emphasized with the gray dashed line.

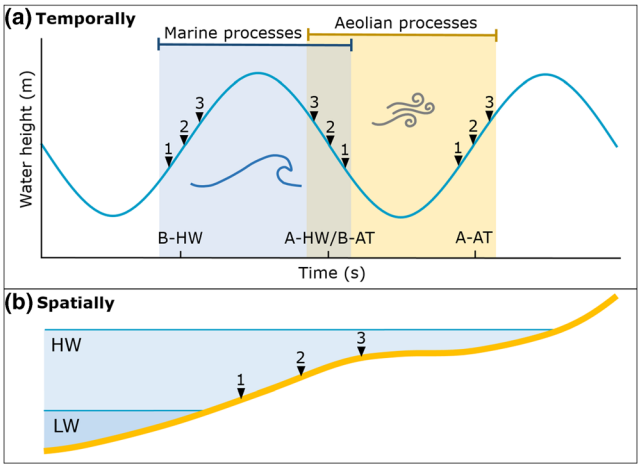

FIGURE 6 Conceptual representation of the spatial and temporal sampling strategy that was used to assess the vertical variability of the grain size distribution in the intertidal zone on the intratidal timescale. Black triangles indicate times and locations at which the vertical grain size distribution is sampled. (a) The impact of the marine processes on the vertical grain size variability (blue shaded area) is determined by sampling the bed surface before high water (B-HW) and after high water (A-HW). The inundation during high water could be caused by high tide, storm surge, wave setup, and/or swash. The influence of the aeolian processes (yellow shaded area) is determined by sampling before aeolian transport (B-AT) and after aeolian transport (A-AT), possibly during a low water. (b) Three locations in the intertidal zone, between low water (LW) and high water (HW), are sampled to get an indication of the cross-shore variability in the vertical grain size layering. Each sampling location has a different elevation so they are each exposed and submerged at different times in the tidal cycle. Thus, the sampling time depends on the sampling location, as indicated by the corresponding numbers between subplot (a) and (b).

Additionally, the most landward sampling location should be at a low enough elevation to be impacted during high water. Wind predictions, water level predictions, measurements of the maximum runup during the preceeding high tide and visual cues in the field (e.g., the wreck line and berm location) were used to determine the most favorable sampling moment and locations.

Since the sand scraper is an intrusive sampling method, consecutive samples (in time) from the same reference cross-shore location were taken approximately 1–3 m apart in the alongshore direction. real time kinematic global positioning system (RTK GPS) measurements were collected to determine the exact horizontal and vertical coordinates of each sampling location. Alongshore grain size variability can be expected due to, for instance, aeolian sand strips (Hage et al., 2018; Nield et al., 2011), rips (Gallagher et al., 2011), and lag deposits (Zhenlin Li & Komar, 1992). Thus, the applied alongshore spacing could introduce deviations between consecutive samples that are not related to the temporal signals driven by waves and winds but related to the local alongshore variability. For this study, we initially assume that the signals related to the temporal signals dominate over the local alongshore variability.

Additionally, the sand scraper requires insertion into the bed surface. This invasive process may disturb the near-surface sediments by pushing them upwards, leading to some uncertainty in the precise depth below the surface at which sediment samples are collected. In cases where these disturbances occurred, the maximum vertical deviation is estimated to be around 2 mm. This can translate to vertical deviations between the depth of layers in samples that were collected at the same cross-shore location, but at different times (and thus different alongshore locations). However, these possible vertical deviations are limited, so temporal trends in the vertical variability of the grain size distribution are expected to be visible despite them.

2.4 | Topographic surveys

At every field site, topographic surveys of the subaerial beach profile were conducted. These profiles were collected to determine the occurrence of erosion and deposition at the bed surface, as this is crucial to interpret the changes in the vertical variability of the grain size distribution. In Noordwijk and Waldport, RTK GPS transects were measured, and in Duck bed elevation data from a co-located continuously scanning terrestrial laser scanner were used (O'Dea et al., 2019). The elevations in the United States were measured relative to NAVD88 and in the Netherlands relative to NAP. The error margin of the GPS measurements was in the order of 0.01–0.02 m. The largest changes in elevation occurred due to marine processes, so most profiles were measured before and after high water. In Waldport and Noordwijk, the cross-shore location of the maximum swash excursion was measured to indicate the extent of the marine processes during high water. The elevation changes due to the formation of depositional patterns during aeolian sediment transport were often within the error margin of the survey methods. Thus, during experiments where the initiation of these patterns was expected/observed, erosion pins were used to provide a more detailed indication of erosion and deposition.

2.5 | Experiment specifications

A total of nine experiments were conducted divided over the three field sites (Table 2), resulting in 400+ individual samples. During most of the experiments, samples were collected to determine the effect of both marine and aeolian processes on the vertical variability of the grain size distribution (according to the sampling strategy in Figure 6). Additional samples were collected to evaluate the sampling method and to determine the effect of spatial variability.

The repeatability of the developed sand scraper sampling method was tested in Duck and Noordwijk by collecting two duplicate samples within 1–2 m distance of each other (repetition sampling, Table 2). By comparing these samples an indication of the extent of inherent variations in grain size and vertical deviations can be given.

The effect of marine and aeolian processes on the vertical variability of the grain size distribution were examined at all three field sites. In Waldport, on August 23. 2021 (Table 2), samples were collected in the intertidal zone before and after high water (B-HW and A-HW/B-AT, Table 3). Subsequently, aeolian transport occurred during low water. However, during this event, aeolian transport was limited (see wind event described in Table 4). Thus, sampling after aeolian transport (A-AT) was only carried out at the most landward location where sediment transport had been observed. At this

TABLE 2 Detailed overview of the field experiments. The sampling type indicates whether the samples were collected to determine the effects of marine and aeolian processes (Marine and aeolian), cross-shore variability (Cross-shore), local influence of bedforms (Bedform), or local/background variability (Repetition). The sampling times include the exact timing and the abbreviation that refers to Figure 6(a); before high water (B-HW), after high water (A-HW), before aeolian transport (B-AT), during aeolian transport (D-AT) and after aeolian transport (A-AT)

Field site	Sampling type	Date	Sampling times
Waldport	Marine and aeolian	August 23, 2021	11 a.m. (B-HW), 6 p.m. (A-HW/B-AT) and 9 p.m. (A-AT)
	Bedform	August 23, 2021	9 p.m. (A-AT)
Noordwijk	Marine	February 5, 2020	8 a.m. (B-HW) and 4 p.m. (A-HW)
	Marine and aeolian	January 21, 2021	4 a.m. (B-HW), 1 p.m. (A-HW/B-AT) and 6 p.m. (A-AT)
	Repetition	November 21, 2020	3 p.m.
Duck	Aeolian	September 1, 2021	8 a.m. (B-AT), 2 p.m. (D-AT) and 5 a.m. (A-AT)
		September 2, 2021	
	Marine	September 2, 2021	8 a.m. (B-HW, September 2, 2021), 10 a.m. (A-HW, September 3, 2021)
		September 3, 2021	
	Cross-shore	September 2, 2021	8 a.m.
	Repetition	September 1, 2021	9 a.m.

TABLE 3 Description of the high-water events during which samples were collected with the sand scraper

Event	Wave height (m)	Tidal range (m)	Maximum water level (m)	Storm surge
Waldport August 23, 2021	1.6[a]	1.5[b]	2.0[b]	–[c]
Noordwijk February 5, 2020	1.0[d]	1.3[e]	0.5[e]	–
Noordwijk January 21, 2021	3.4[d]	1.3[e]	1.3[e]	avgerage 0.4 m maximum 1 m[e]
Duck September 2, 2021 peak from 4 p.m. to 1 a.m.	1.3[f]	0.8[g]	1.4[g]	0.3 m[g]

[a]Wave height from NOAA station 46098 offshore of Newport.
[b]Predicted value from NOAA station 9434939 in Waldport.
[c]No storm surge expected based on measurements at nearby stations.
[d]Euro platform offshore of Noordwijk.
[e]Scheveningen water level station.
[f]NOAA station 44056 offshore of Duck.
[g]NOAA station 8651370 on FRF pier.

TABLE 4 Description of the three wind events that resulted in aeolian transport during which sample samples were collected with the sand scraper

Event	Wind direction	Average wind speed (m/s)	Wind gusts
Waldport[a] August 23, 2021	Alongshore winds, slightly onshore	7	Up to 12.5 m/s
Noordwijk[b] January 21, 2021	Alongshore winds, slightly offshore	14	Up to 23 m/s
Duck[c] September 1, 2021 peak from 12 a.m. to 6 p.m.	Alongshore winds, slightly onshore	7	Around 12 m/s, up to 15 m/s

[a]NOAA station 9435380 in Newport.
[b]KNMI station in Hoek van Holland.
[c]Measured at 5.5 m above the dune.

location, bedforms occurred during the event. Samples were collected on the crest and in the trough of the bedform to determine spatial variations in grain size.

In Noordwijk, on February 5, 2020, samples were collected before and after high water (B-HW and A-HW) to determine the effect of marine processes on the vertical variability of the grain size distribution (Tables 2 and 3). On January 21, 2021, samples were again collected before and after high water (B-HW and A-HW/B-AT) followed by sampling after aeolian transport (A-AT), which had occurred during low water. The high-water event was associated with relatively large waves and a surge that was largest before high tide but reduced to 0.4 m around the high tide peak (Table 3). The wind event that caused the aeolian transport was intense with large amounts of transport (Table 4).

In Duck, sampling took place during a wind event and storm surge event related to remnants of Hurricane Ida as it passed along the east coast of the United States (Beven et al., 2022). Samples were collected to determine the effect of both marine and aeolian processes on the vertical variability of the grain size distribution. The samples were collected before, during, and after aeolian transport (B-AT, D-AT, and A-AT) that occurred during the peak of the wind event on September 1, 2021 (Table 4). The vertical variability of the grain size distribution measured after the aeolian transport event was supplemented with beach surface samples down to 8 mm depth along an array with a cross-shore spacing of 1–2 m. The purpose of this experiment was to get a more detailed indication of the cross-shore gradients in grain size that were present in Duck, which were not fully captured by the three cross-shore sample locations.

The winds continued after September 1, 2021 but they were not strong enough to cause aeolian transport. However, during the daytime of September 2, 2021, the wind got a more onshore directed component, which resulted in a surge of approximately 0.3 m along the coast (Table 3). Samples were collected before and after the storm surge (B-HW and A-HW) to determine the effects of this high-water event on the grain size distribution.

3 | RESULTS

In this section, the observed spatio-temporal patterns and vertical grain size variability in Waldport, Duck, and Noordwijk are presented. Initially, the repeatability of the new sampling method is shown. Then, each sampling occasion that provides insight into the marine and aeolian processes on the vertical variability of the grain size distribution is shown per field site. For most of the sampling locations, a comparison is made between the grain size distribution in each layer and the $ø_{50}$ (weighted average median grain size of all layers in a cross-section) to provide insight into the comparison between bulk sampling and sampling with the sand scraper. Additionally, locations are pointed out where the vertical grain size variability could have an effect on the sediment availability for aeolian sediment transport. To provide insight into the spatial variations in the vertical grain size layering, the spatial variability due to bedforms in Waldport, and the spatial variability due to cross-shore gradients in Duck are discussed.

3.1 | Repetition samples

Repetition samples were collected in Noordwijk and Duck to determine local grain size variability at the beach surface, and assess the repeatability of the new sampling method (Figure 7). Here, we qualitatively compare the two adjacent samples that were taken at each field site. The samples from Noordwijk showed a comparable gradient with finer sand on top of coarser sand. However, there was a vertical shift in the boundary between the finer and coarser sand (dashed line in Figure 7). Possibly, the layer at 14 mm depth for Noordwijk 2 consisted of a mixture of the layers at 8 and 14 mm in Noordwijk 1, which would explain the intermediate grain size. In that case, the vertical deviation is smaller than 6 mm. Correcting for this vertical shift, corresponding layers from the two sample locations displayed minor deviations in median grain size, ranging from 5 to 15 µm. The repetition samples from Duck, show similar variations in vertical grain size as those from Noordwijk. Perhaps, the gradient from the surface down to 38 mm in Duck 1, where there is first fining and then coarsening, corresponds to the gradient down to 26 mm depth in Duck 2 (dashed line in Figure 7). The averaged median grain size, $ø_{50}$, varied in the order of 5 µm and the vertical deviation is in the order of 6 mm.

3.2 | Measured spatial and temporal variations in Waldport

The influence of marine and aeolian processes on the vertical grain size variability in Waldport was investigated through repeated sampling before high water (B-HW) and after high water (A-HW/B-AT),

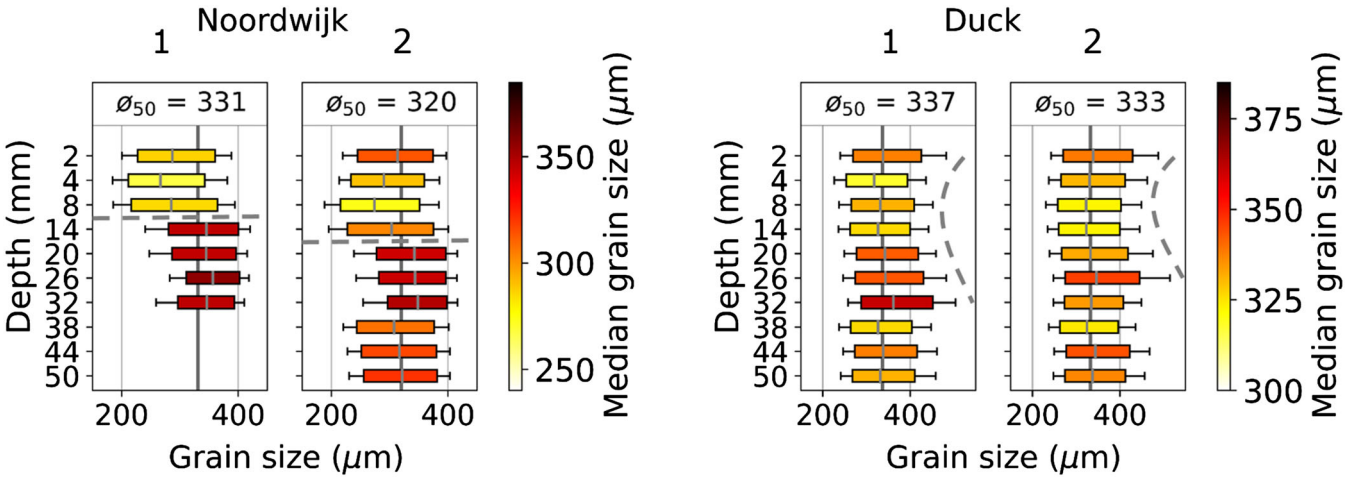

FIGURE 7 Vertical variability of the grain size distributions measured on November 21, 2020 in Noordwijk, and September 2, 2021 in Duck. Colors indicate the median grain size. Box plot dimensions are based on the D_{25} and D_{75}, and the extent of the whiskers on the D_{16} and D_{84}. The $ø_{50}$ indicates the averaged D_{50} in micrometers. At each field site, two samples were collected within 2 m of each other. The dashed gray lines indicate comparable trends that are present in the samples of each field site. For Noordwijk, the dashed gray lines emphasize a boundary between fine and coarse sediment which occurs in both samples, and for Duck they emphasize a vertical gradient that occurs in both samples.

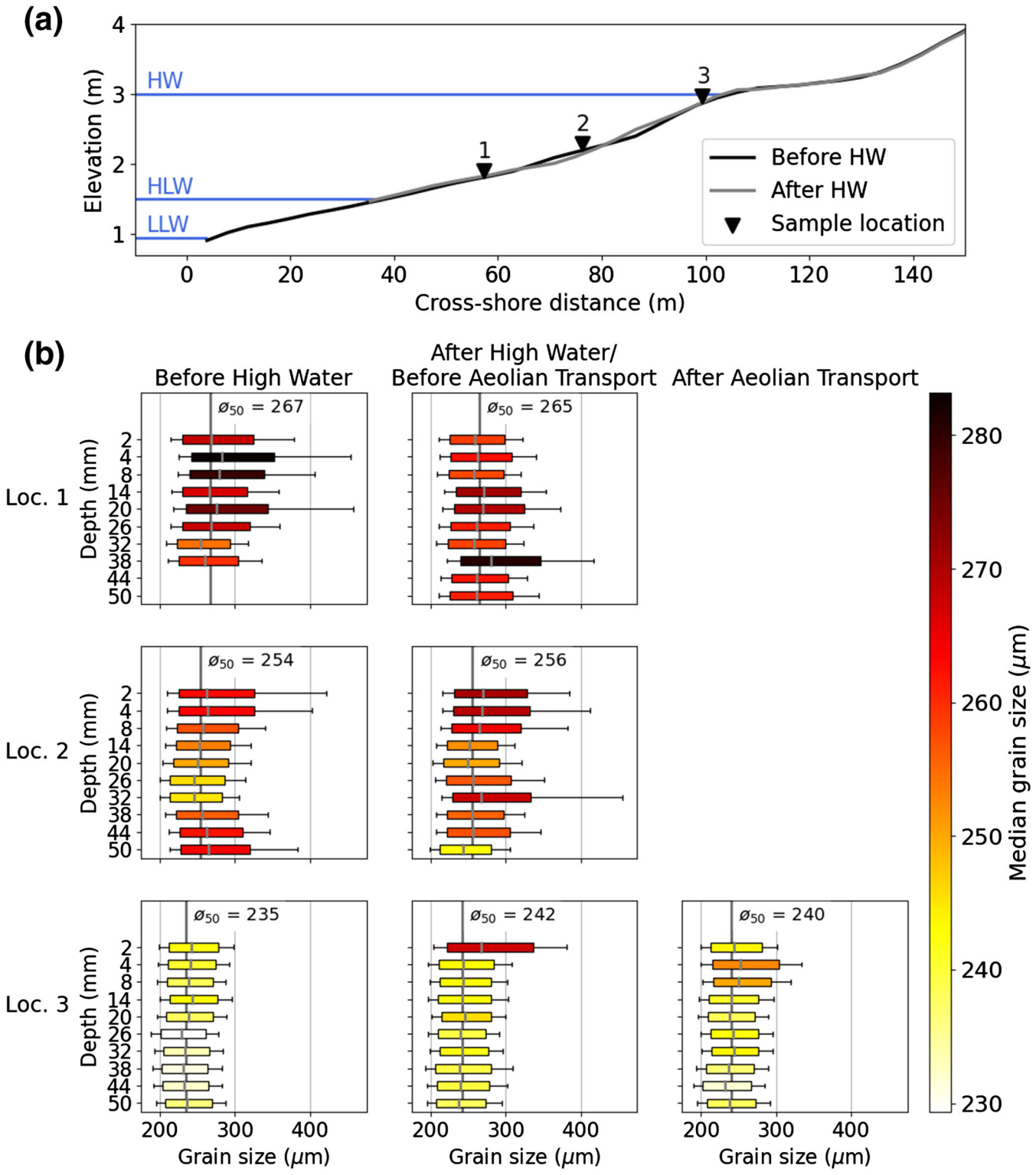

FIGURE 8 Overview of transects and the vertical variability of the grain size distributions measured on August 23, 2021 in Waldport. (a) Cross-shore profiles measured before (black) and after (gray) high water (HW). The upper blue line indicates the maximum swash excursion during high tide. The two lower blue lines indicate the low low water (LLW) that occurred before the HW and the high low water (HLW) that occurred after the HW. Sample locations are indicated by black triangles. (b) Vertical grain size distributions sampled before high water (B-HW), after high water (A-HW/B-AT) and after aeolian transport (A-AT) which occurred during the subsequent low water. Colors indicate the median grain size. Box plot dimensions are based on the D_{25} and D_{75}, and the extent of the whiskers on the D_{16} and D_{84}. The $ø_{50}$ indicated by the dark gray vertical line represents the averaged D_{50} in micrometers. Location numbers correspond to the locations in (a).

and after aeolian transport (A-AT) (Figure 8). After aeolian transport, sampling was only repeated at Location 3, since this was the only location with observed transport. Data were collected down to 50 mm at all sample locations in Waldport except at Location 1, where layers were only collected down to 32 mm due to rising tides during the B-HW collection.

Distinct spatial variations were visible in the vertical variability of the grain size distributions sampled from Location 1 (lower intertidal

zone) to Location 3 (upper intertidal zone). The averaged median grain size, $ø_{50}$, decreased in the landward direction (Figure 8). Additionally, the grain size distribution was most narrow and the D_{50} per layer resembled most closely the $ø_{50}$ for Location 3. In contrast to Location 1, where the vertical variability in the grain size distribution was the most heterogeneous, with the D_{14} and D_{86} covering a range from 210 to 460 μm.

The total water level covered all three sample locations between the B-HW and A-HW collections, and all locations showed a change in the vertical variability of the grain size distribution A-HW compared to B-HW. At Location 1, the D_{84} showed less peaks above 400 μm, and finer sand was available at the surface after high water, indicating that the sediment availability for aeolian transport might have increased. Before high water (B-HW), Location 2 showed fining downwards down to 32 mm depth, and coarsening in the deeper layers. This gradient was not as distinct after high water and larger variations in grain size occurred. This change in the vertical grain size variability is probably related to the morphological change (approximately 0.05 m of erosion) that occurred at this location (Figure 8a). Location 3 was influenced by only several swash excursions. In the 2 mm thick surface layer, the median grain size increased from 242 to 267 μm after the high water. Below the upper layer, there were small changes (order of 10 μm) in the vertical variability of the grain size distribution A-HW compared to B-HW. Given the lack of marine influence at the upper limit of the intertidal zone, these variations are more likely to be related to natural spatial variations in grain size than the effect of marine processes.

At Location 3, a 2 mm layer of finer sand was present on top of coarser material (2–8 mm depth) after the aeolian transport event (A-AT). The coarser material is probably related to the coarse deposit seen in the upper 2 mm A-HW. Potentially, there was a different distribution of the coarse layer between the sampling layers of the sand scraper resulting in the inclusion of more fine sediment in the samples and thus more moderate grain sizes. Four erosion pins were used in the field within 2 m of Location 3 during the aeolian transport event, which showed accretion in the order of 3 to 9 mm. Thus, it seems that the coarse bed surface was buried with a thin layer of fine sediment. This deposition might have been related to a meter-scale bedform that formed during the aeolian transport. Samples from the crest and in the trough of the bedform (Figure 9) show that the vertical grain size layering of the crest consisted of a 2 mm thick, fine sand layer on top of downward fining sediment. This downward fining gradient is also visible in the cross-section from the trough; however, the fine sediment layer on top is not present.

3.3 | Measured spatial and temporal variations in Noordwijk

In Noordwijk, the vertical grain size variability due to the influence of marine processes was studied by sampling before high water (B-HW) and after high water (A-HW) on February 5, 2020 (Figure 10). In both the B-HW and A-HW samples, the coarsest grain sizes were found on the landward side of the coastal profile (Location 3), but the $ø_{50}$ of Locations 1 and 2 did not show a distinct cross-shore trend.

For Location 1, the vertical grain size layering was reversed after high water, with fine sand on top instead of in the deeper layers as before the high water. Despite this clear change in the vertical layering, the $ø_{50}$ remained approximately the same. Thus, a bulk sample would have shown a relatively small change in grain size, whereas the vertical layering shows an increase in the availability of fine sand near the surface. The coastal profiles (Figure 10a) show that the bar moved landward (cross-shore distance = 20 m), corresponding to elevation changes up to 0.1 m and, thus, indicating mobilization of a considerable amount of sediment around Location 1. This is in contrast to Location 3, where the calculated elevation change for Locations 2 and 3 was around 0.005 m, which was within the error margin of the GPS measurements. At this Location, only the upper limit of the gradient (dashed gray line in Figure 10) showed an upward 6 mm shift and the layers beneath that a shift of up to 18 mm.

On January 21, 2021, a second field experiment was completed in the intertidal zone of Noordwijk. Samples were collected before and after high water (B-HW and A-HW/B-AT) and after the

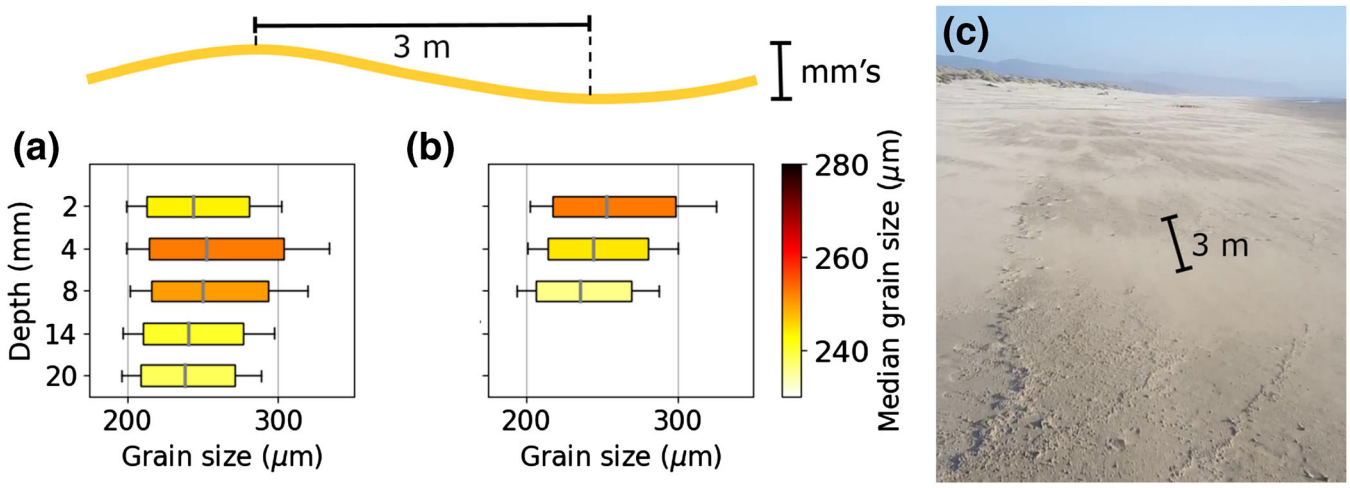

FIGURE 9 Schematic representation of a meter-scale bedform with a height in the order of millimeters and the vertical variability of the grain size distributions in its crest (a) and trough (b) as measured on August 23, 2021 in Waldport. The bedform occurred on the landward end of the intertidal zone after a period of aeolian transport, as shown in (c). Colors in (a) and (b) indicate the median grain size. Box plot dimensions are based on the D_{25} and D_{75}, and the extent of the whiskers on the D_{16} and D_{84}.

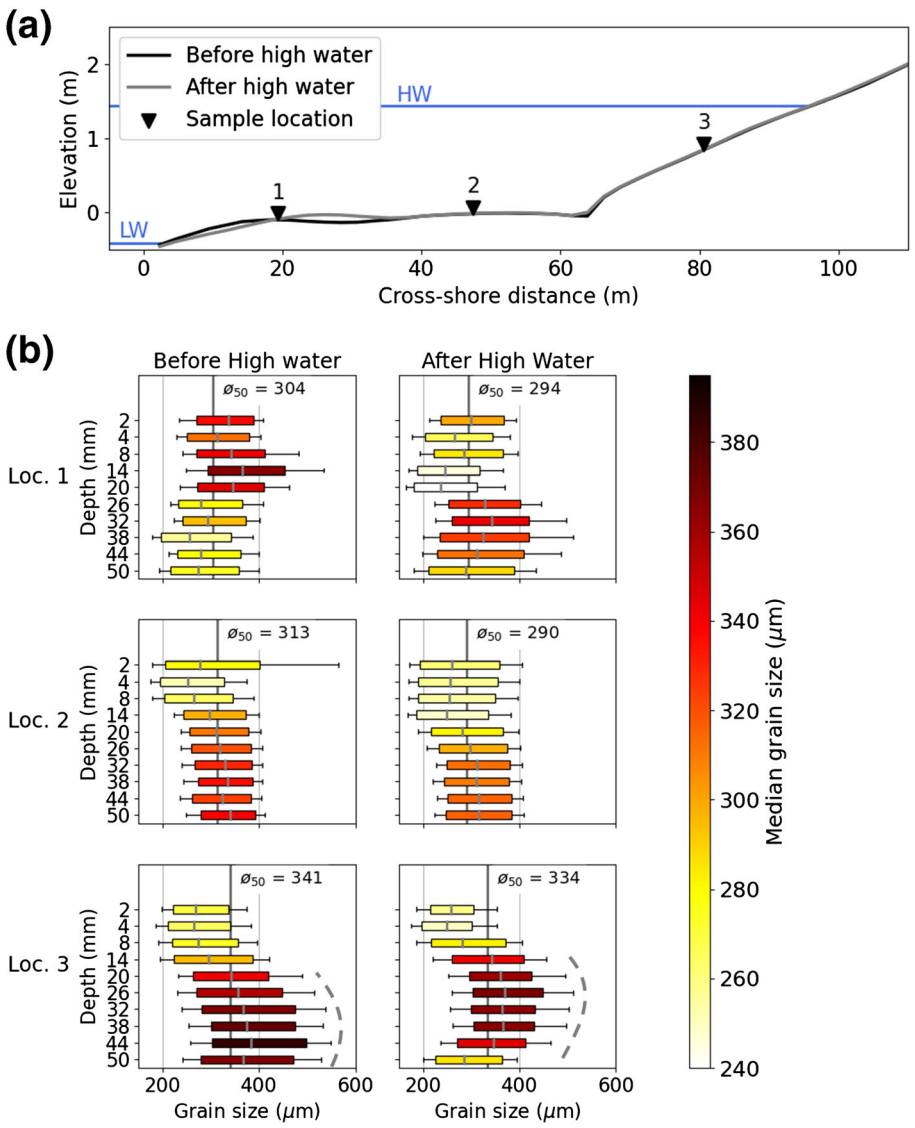

FIGURE 10 Overview of transects and vertical variability of the grain size distributions measured on February 5, 2020 in Noordwijk. (a) Cross-shore profiles measured before (black) and after (gray) high water. The upper blue line indicates the maximum swash excursion during high tide. The lower blue line indicates the low water (LW) elevation. Sample locations are indicated by black triangles. (b) Vertical grain size distributions sampled before high water (B-HW) and after high water (A-HW). Colors indicate the median grain size (D_{50}). Box plot dimensions are based on the D_{25} and D_{75}, and the extent of the whiskers on the D_{16} and D_{84}. The $ø_{50}$ indicated by the dark gray vertical line represents the averaged D_{50} in micrometers. Location numbers correspond to the locations in (a). The dashed gray lines emphasize a comparable vertical gradient that was present in the samples from B-HW and A-HW at Location 3.

occurrence of aeolian transport (A-AT) during low water when a wind event occurred (Figure 11). Large amounts of transport were observed during the field data collection period (see conditions in Table 4). Thus, even when the A-HW/B-AT sampling was executed within an hour of the water receding, aeolian transport was already occurring. For Location 2, the exposure to aeolian transport was approximately half an hour, and for Location 3, 1 h. Similarly, the GPS transect measured after high water (Figure 11a, gray line) can also include some elevation changes due to aeolian transport that occurred. It was collected around low water when the profile had already been affected by aeolian sediment transport.

The largest change in the vertical variability of the grain size distribution after the high-water event can be seen at Locations 1 and 3 (Figure 11b). Before high water, the vertical grain size variability at Location 3 was relatively uniform, with an averaged median grain size of 281 μm. However, after high water, a 14 mm thick layer of finer sand (255 μm) covered a layer of coarser sand (298 μm). This vertical layering, indicated by a dashed gray line in Figure 11(b), is not shown by the change in $ø_{50}$ (from 281 μm B-HW to 285 μm A-HW). This change in the vertical variability of the grain size distribution at Location 3 corresponded to a considerable change in morphology (Figure 11a). At Location 1, comparable downward coarsening gradients were present in the sediment B-HW and A-HW (dashed gray lines in Figure 11b). However, the lower limit of this gradient, defined here as the coarsest grain size present, became 12 mm deeper. Changes at Location 2 were relatively small, although the difference in grain size between the upper and lower layers became more pronounced (dashed gray line in Figure 11b). This resulted in a 7 μm increase of the $ø_{50}$, although the grain size in the upper layers decreased.

The vertical variability of the grain size distribution changed considerably after the aeolian transport in Locations 2 and 3. During the aeolian transport, meter-scale bedforms were migrating past Locations 2 and 3. On the contrary, Location 1 did not show any major changes, and no clear bedforms were present. At Location 2, the vertical grain size variability became more uniform, with relatively fine sand compared to the other sampling locations and times. This might be related to the presence of aeolian deposits related to the bedforms that had an elevation in the order of millimeters to centimeters (based on measurements with erosion pins). At Location 3, finer sand (256 μm) was present in the upper 14 mm before aeolian transport (dashed gray line in Figure 11b). After aeolian transport, Location 3 was located outside of a depositional patch. The layer of finer sand was no longer present, and the grain size of the upper 14 mm

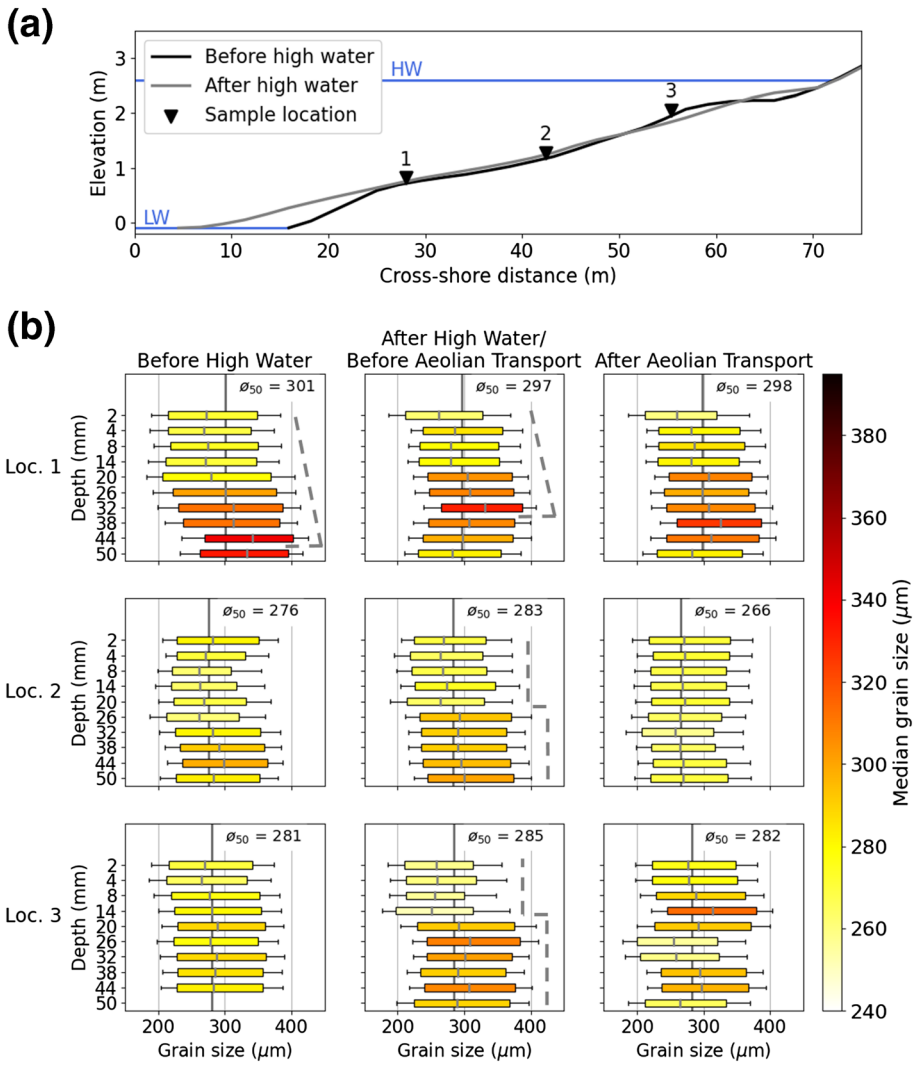

FIGURE 11 Overview of transects and vertical variability of the grain size distributions measured on January 21, 2021 in Noordwijk. (a) Cross-shore profiles measured before (black) and after (gray) high water. The upper blue line indicates the maximum swash excursion during high tide. The lower blue line indicates the low water (LW) elevation. Sample locations are indicated by black triangles. (b) Vertical grain size distributions sampled before high water (B-HW), after high water (A-HW/BAT) and after aeolian transport (AAT) which occurred during the subsequent low water. Colors indicate the median grain size. Box plot dimensions are based on the D_{25} and D_{75}, and the extent of the whiskers on the D_{16} and D_{84}. The $ø_{50}$ indicated by the dark gray vertical line represents the averaged D_{50} in micrometers. Location numbers correspond to the locations in (a). The dashed gray lines in the vertical distributions of Location 1 emphasize a coarsening downward gradient that was present both B-HW and A-HW. The dashed gray lines in the vertical distributions of Locations 2 and 3 emphasize a boundary between finer sediment and coarser sediment that is present A-HW/B-AT at both of these locations.

increased to 289 μm. This could indicate that erosion of the fine sediment occurred during aeolian transport.

3.4 | Measured spatial and temporal variations in Duck

On September 1, 2021, three locations on the dry beach in Duck were sampled (Figure 12). They were located above mean high water on a flat berm susceptible to inundation during storms (Figure 12a). The sampling on September 1, 2021 was repeated before, during, and after the aeolian transport event (B-AT, D-AT, and A-AT), during a period where none of the three locations were inundated. The measured vertical variability of the grain size distributions showed vertical gradients but no clear spatial or temporal coherence (Figure 12b).

Overall in Duck, no clear temporal trend was visible in the vertical grain size variability of each location between the B-AT, D-AT, and A-AT sampling times. Still, there are large variations visible between the different times of each location, as indicated by variability in the $ø_{50}$ and changes in the apparent vertical distributions of grain size (Figure 12b). The LiDAR-derived topography data (Figure 12a) indicates that there was < 0.01 m of vertical change at all sampling sites over this period. Given these small net variations, limited observations of aeolian bedforms, and the absence of marine processes at the sampling locations, the observed temporal variability is presumed to reflect alongshore spatial variations more so than changes due to the occurrence of aeolian transport.

In the cross-shore, the averaged median grain size, $ø_{50}$, for Location 1 (most seaward) was finer than those at Locations 2 and 3 (most landward). However, due to the large grain size variability, no clear cross-shore trend was present (Figure 12). Cross-shore sampling with decreased horizontal spacing (1–2 m compared to 4–6 m) was executed after the aeolian transport event (A-AT) (Figure 13). At this resolution, there was still significant vertical variability in the grain size distribution but an increase in grain size in the landward direction was visible.

After the aeolian transport event, the wind became more onshore directed, which contributed to a storm surge of approximately 0.3 m along the coast (Table 3). Several locations were sampled before inundation (B-HW) and after inundation (A-HW) to determine the effect of marine processes (Figure 14). During the high-water event, considerable erosion occurred, which resulted in the formation and landward movement of a beach scarp (± 0.2 m high, Figure 14a). Before inundation, Location 1 was on the dry beach near the most landward edge of the intertidal zone. After inundation, the scarp had formed and retreated landward of Location 1, resulting in bed lowering at Location 1 and marine inundation during high tide. At this point, Location

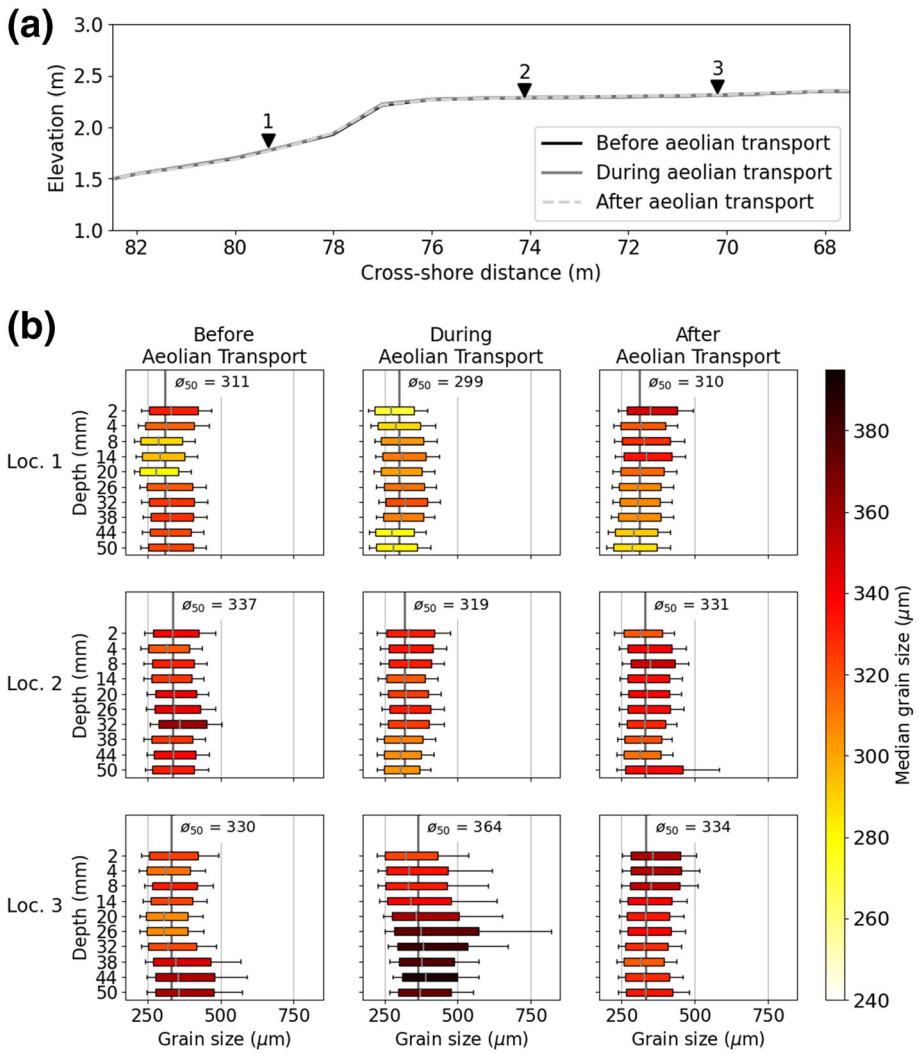

FIGURE 12 Overview of transects and vertical variability of the grain size distributions measured on September 1, 2021 and September 2, 2021 in Duck. (a) Cross-shore profiles measured before (black), during (gray), and after (gray, dashed) aeolian transport. (b) Vertical variability of the grain size distributions sampled before (B-AT), during (D-AT) and after aeolian transport (A-AT). Colors indicate the median grain size. Box plot dimensions are based on the D_{25} and D_{75}, and the extent of the whiskers on the D_{16} and D_{84}. The $ø_{50}$ indicated by the dark gray vertical line represents the averaged D_{50} in micrometers. Location numbers correspond to the locations in (a).

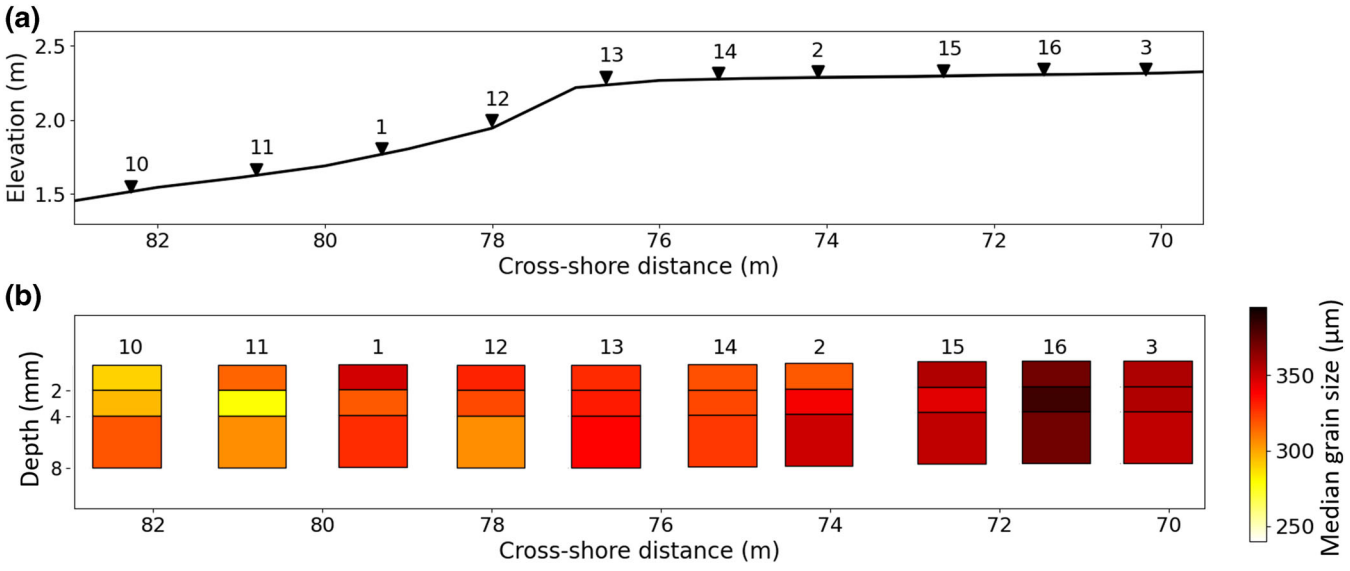

FIGURE 13 Overview of transect and vertical variability of the grain size distributions measured on September 2, 2021 in Duck. (a) Cross-shore profile based on laser scan with sampling locations indicated by black triangles. (b) Vertical grain size variability sampled after aeolian transport. Colors indicate the median grain size. Location numbers correspond to the locations in (a).

12 became the most seaward point landward of the scarp. During the high tide of the high-water event, this location was influenced by some wave runup.

The vertical grain size variability in the intertidal zone changed considerably where erosion occurred during the high-water event (Figure 14b). The most seaward location (Location 10), showed

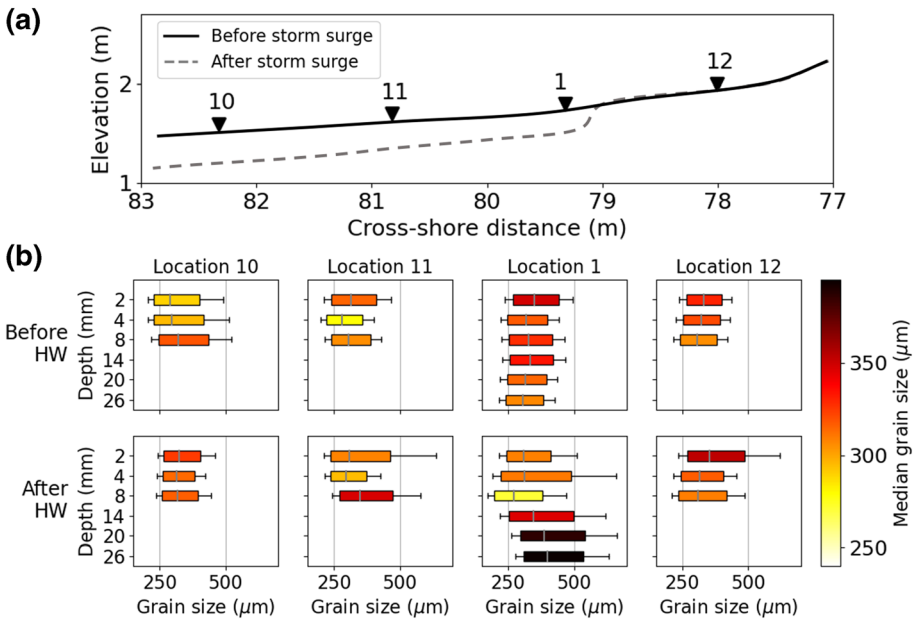

FIGURE 14 Overview of transects and vertical variability of the grain size distributions measured on September 2, 2021 and September 3, 2021 in Duck. (a) Cross-shore profile based on laser scans and sketches from before (black) and after (gray, dashed) a storm surge occurred. (b) Vertical variability of the grain size distributions sampled before marine (B-HW) processes and after marine (A-HW) processes occurred due to the storm surge. Colors indicate the median grain size. Box plot dimensions are based on the D_{25} and D_{75}, and the extent of the whiskers on the D_{16} and D_{84}. Location numbers correspond to the locations in (a). Location 1 corresponds to Location 1 in Figure 9. The sampling before marine processes occurred after aeolian transport (A-AT), which corresponds to Figure 9.

downward coarsening in grain size before inundation, which changed into a downward fining gradient. Although, these additional samples had a maximum depth of 8 mm, which is far smaller than the total net erosion (up to 0.2 m) in this zone.

The vertical gradient in the grain size distribution at Location 12 kept fining downwards, although the range between the D_{14} and D_{86} became larger A-HW compared to B-HW. Especially, the surface layer became coarser which may be related to swash-related sediment transport that occurred at this location. In contrast, Locations 11 and 1, where the scarp moved landward, showed more substantial changes. Both locations changed from a vertical layering with the coarsest grain sizes on top to coarse sediment overlain with a 4–8 mm thick layer of fine sand. Based on visual inspection, the coarse material measured after inundation at 8 mm depth for Location 11, and 14 mm depth for Location 1 continued for at least several centimeters into the bed.

4 | DISCUSSION

A newly developed sand scraper was used to measure vertical grain size variability in the intertidal area at Waldport, Noordwijk, and Duck. Based on these case studies, we discuss to what extent marine and aeolian processes influenced the observed grain size variability and sediment availability for aeolian transport at the three field sites. Additionally, we discuss the applicability of the new sand scraper sampling method, and how the findings collected with the sand scraper can inform future research and modeling.

4.1 | Observed spatial grain size variability

In agreement with previous studies (e.g., Çelikoğlu et al., 2006; Stauble & Cialone, 1997), cross-shore gradients in grain size were observed at all three field sites (Figure 15). The maximum range in the $ø_{50}$ measured horizontally between sampling locations was 32 μm for Waldport, 51 μm for Noordwijk and 65 μm for Duck. The data collected in Duck indicates that there can be alongshore variations in grain size that have a similar magnitude as the cross-shore variations, even at alongshore distances < 10 m. The longshore variability of grain size at Duck might be related to alongshore morphological features, such as beach cusps, or bioturbation due to ghost crab burrowing (Chakrabarti, 1981; Schlacher et al., 2016). Additionally, the considerable spatial grain size variation at Duck could be related to the wide grain size distribution that is present at this field site.

Despite this large heterogeneity in sediments alongshore at Duck, there was a clear cross-shore gradient in grain size when additional locations were added to increase spatial resolution. This indicates that more spatially frequent sampling may be required to characterize the full heterogeneity of the spatio-temporal grain size dynamics of the bed. Combining the sand scraper with other grain size measurement methods could provide a viable solution. We especially recommend this approach for intermediate, mixed grain beaches where considerable spatial grain size variations could be expected.

4.2 | Observed temporal grain size variability

By using the sand scraper, this study could show the detailed grain size layering at the bed surface and how it changed through time due to marine and aeolian processes. The most distinct temporal variations occurred where there was a significant morphological change after a high-water event. This is consistent with studies from other field sites, which have attributed changes in grain size of the bed surface within the intertidal zone to sediment advection and sediment mixing due to, for instance, sandbar, bedform and berm migration (e.g., Gallagher et al., 2011; Jackson & Nordstrom, 1993; Medina et al., 1994; Sherman et al., 1993; Sonu, 1972).

The measurements show that marine processes resulted in fining of the surface sediments in several cases. At the Noordwijk site Location 1 in Figure 10, a bed of fine sand overlain with coarser sand before the high tide changed into coarse sand overlain with finer sand after the high tide. Similar trends were noted at both Location 3 in Figure 11 (Noordwijk) and Location 1 in Figure 14 (Duck), where

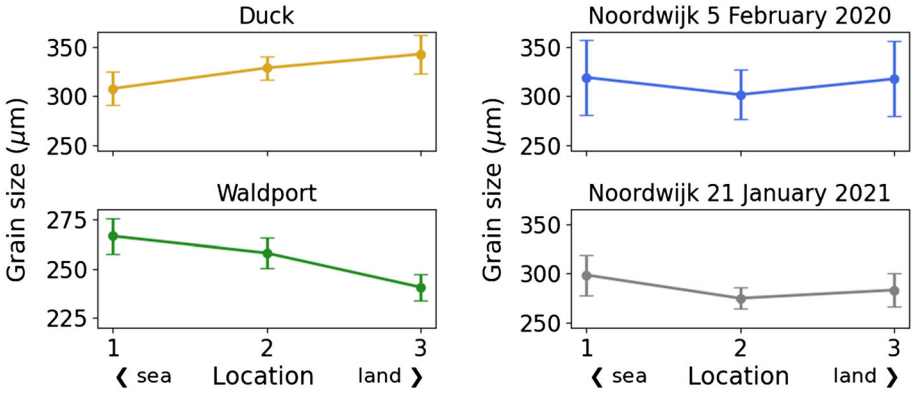

FIGURE 15 Overview of the cross-shore gradients in grain size and the associated standard deviation (shown as error bars), calculated as the temporally averaged $ø_{50}$ and standard deviation per field site, respectively. The cross-shore and marine sampling from Duck were excluded due to the limited sampling depths. Note that the sampling locations (Locations 1, 2, and 3) belonging to each panel (i.e., each sampling occasion) are not necessarily in similar locations along the coastal profile. However, Location 1 is always on the seaward side (sea) and Location 3 is always on the landward side (land), indicated by the arrows.

temporal fining occurred. In these cases, the contrast between the upper finer and the lower coarser layers increased after the high-water event. The measured morphological change at these sampling locations was typically small, < 0.1 m, except in the case at Duck. Still, the changes in the intertidal profile indicated that a combination of both sediment advection and mixing likely had occurred. Based on the available data, the exact hydrodynamic mechanisms that affected sediment redistribution within the intertidal zone cannot be determined. However, the results indicate that marine processes can be an important means of introducing fine sediments to the bed surface.

Meanwhile, other observations indicate that the marine processes can also result in coarsening of surface sediments. There were two cases where the surface layer changed and became coarser after the high water at the upper portion of the intertidal zone, in Waldport Location 3 in Figure 8 and Duck Location 12 in Figure 14. In the Waldport case, it appears that a thin veneer of coarser grains was deposited directly on top of the fines. Bauer (1991) observed a similar veneer and related it to a large wave's swash excursion that occurred during high tide. According to Bauer (1991), the coarse sand was transported by the uprush, followed by rapid deposition as considerable infiltration reduced the flow during the downrush. A different formation mechanism was given by Clifton (1969) and Sallenger (1979), who described how vertical segregation of grains during wave backwash can result in lamination with coarse grains near the surface. In this research, the specific explaining mechanism is unclear. However, both occasions of near-surface coarsening that were recorded were located near the upper limit of wave runup during high tide, indicating that formation of the coarse layer could indeed be related to the backwash that occurred during receding tide. In summary, the results show that marine processes alter grain size variability and that these processes, depending on which small-scale processes are occurring and which antecedent bed composition is present, may lead to either coarsening or fining of the surface sediment.

When considering aeolian sediment transport, the surface layer was expected to become coarser due to grain size-selective pickup by the wind. However, the observations following aeolian transport events saw both coarsening and fining of the bed surface. At Noordwijk Location 3 in Figure 11, the grain size in the surface layer coarsened after an aeolian transport event, possibly due to the removal of fine sand. In contrast, there were two occasions, Waldport Location 3 in Figure 8 and Noordwijk Location 2 in Figure 11, where the grain size in the surface layer decreased. The decrease in grain size was associated with an increase in the bed elevation, indicating deposition of aeolian transported sediment. The deposition in Waldport occurred during conditions with alongshore winds that caused meter-scale bedform formation (Figure 9). On the crest of the bedform, fining of the bed surface occurred, while coarser sediment was present in the surface layers of the trough. The observations show that fine sediment, which increases the sediment availability, could be supplied to the intertidal zone from upwind areas during aeolian transport events.

4.3 | Implications for sediment availability for aeolian transport

Aeolian transport rates are influenced by grain size in many ways. In the commonly used aeolian transport equations by Bagnold (1937b), the transport rate, threshold velocity, and parameterization of the bed roughness all depend on the grain size. de Vries et al. (2014) proposed that the intertidal zone is an important source area for aeolian transport towards the dunes. A following study demonstrated wind-induced erosion of about 20 mm/h in the intertidal area during low tide using a terrestrial laser scanner (e.g., de Vries et al., 2017). Thus, the grain size of the upper layers in the intertidal zone is assumed to be important for the sediment supply of aeolian transport towards the dunes.

The observations in this study showed that individual layers could significantly deviate from the vertically averaged median grain size, $ø_{50}$, in the upper 50 mm of the bed surface. If vertical grain size variability were determined based on the $ø_{50}$, it would be assumed that the sediment availability for aeolian sediment transport is uniform in the vertical. Such assumptions could lead to errors because of the strong relationships between grain size and aeolian transport processes. For example, in the case of the Duck measurement campaign the measured D_{50} for Location 1 (A-AT) was 349 μm at 2 mm and 286 μm at 50 mm below the bed surface (Figure 12b), with a $ø_{50}$ of 310 μm. These measurements result in threshold velocities for aeolian

transport of 10.1 m/s, 9.1 m/s, and 9.5 m/s, respectively, as calculated according to Bagnold (1937b) for wind speeds at 2 m above the bed. Since sediment transport rates are commonly expressed as a cubic relation with the threshold velocity (Bagnold, 1937b; Kawamura, 1951; Lettau & Lettau, 1978; Sherman & Li, 2012), differing sediment fluxes may be expected for each of those D_{50} values for the exact same wind speed.

4.4 | Sand scraper methodology advantages and limitations

The sand scraper was developed with the aim to provide a method to determine the vertical variability in grain size at the beach surface, which can impact the sediment availability for aeolian sediment transport. In agreement with previous studies (e.g., Emery, 1978; Masselink et al., 2007), the measurements with the sand scraper showed considerable vertical variability in grain size in the layers that make up the upper 50 mm of the bed surface. The maximum range in D_{50} measured vertically within the top 50 mm was 29 μm for Waldport, 119 μm for Noordwijk and 67 μm for Duck. Specifically, Waldport Location 2 in Figure 8, Noordwijk Location 3 in Figure 10, and Duck Location 1 in Figure 11 all show places where the D_{50} of the individual layers show relatively large deviations from the $ø_{50}$, the average D_{50} of the vertical profile. In these cases, the sand scraper provides detailed information about the bed composition that could not be attained using grab sampling or surface imagery observations.

The sand scraper has some limitations regarding labor intensity, the intrusive nature of the method, and the specific dimensions of the device. Labor intensity limits the applicability of the sand scraper due to the time required to collect (15–30 min per location) and subsequently analyze (multiple hours per location) the grain size of each sample. This makes it difficult to sample over large spatial scales with a high temporal resolution compared to, for example, conventional grab sampling. It is recommended to combine the sand scraper with bulk sampling or photograph-based analysis to, for instance, more clearly distinguish cross-shore grain size trends and sub-hourly temporal developments of the surface grain size. To limit the analysis time of the samples collected with the sand scraper, only their grain size was determined. However, shell content, and mineralogical and density properties can be expected to affect aeolian sediment transport rates. Further analysis that is needed to study these factors would not be possible with, for example, camera imagery, but can be executed on samples collected with the sand scraper due to the direct sampling approach.

However, the intrusive nature of the sampling method limits the application of the sand scraper since sediment is removed from the beach during sampling. Thus, temporal changes in the bed cannot be studied at the exact same location; the sampling needs to be repeated some distance away. Repeatability tests within 1–2 m distance showed that the grain size of corresponding layers between adjacent samples could vary by about 5–15 μm (Figure 7). Part of the variability was associated with vertical offsets in bed layering (relative to the bed surface). However, the observed differences were small enough to compare vertical variability in grain size between repeated samples. Due to the labor intensity of collecting measurements, the repeatability was addressed mostly qualitatively. By executing a focused field effort, more extensive sampling could allow for a more quantitative, statistical analysis of the repeatability in the future.

Lastly, the sand scraper has specific dimensions that limit its application. For example, the scraper takes a discrete set of slices with a minimum resolution of 2 mm. This is suitable for a flat bed of sand-sized sediment (< 2 mm), but these slices might not fully represent larger structures such as wind-driven ripples and shells. Specifically, variations in grain size that occur in wind-driven ripples with coarser grains at the crests and finer grains in the troughs (observed by, e.g., Uphues et al., 2022), would likely not be recorded with the sand scraper sampling methodology. Ripples were not present in the areas sampled in this research. The sampling surface can also be disturbed by shells and coarser grains, causing vertical offsets in the 2 mm thick vertical slices. Thus, a larger layer thickness is recommended when shells or coarse sand are present. Another limiting dimension is the sampling depth limit of 50 mm, which was selected based on the intended purpose of measuring grain size variability at the beach surface to analyze sediment availability for aeolian transport. For applications where sampling to larger depths is needed, the scraper would require a redesign.

While the sand scraper limitations should be taken into account when applying the methodology, the main advantage of the device is that it provides the ability to study the spatial and temporal variations in grain size at a consistent vertical resolution at the sub-centimeter scale that was previously not attainable with, for example, grab sampling and sediment coring.

4.5 | Future measurements and modeling

Most previous studies have inferred changes in sediment availability in the bed from measured changes in sediment fluxes (e.g., de Vries et al., 2014). In contrast, this study focused on resolving changes in bed properties directly by observing changes in grain size distributions in the bed surface. Future studies are expected to focus on additional measurements and modeling of grain size variability.

This study demonstrated significant spatio-temporal variability in grain size in the intertidal zone, both in the vertical and horizontal, which is expected to influence aeolian transport rates. However, the extent to which the changes in vertical grain size variability affect the aeolian transport is still unknown. A combination of both *in situ* measurement techniques for measuring sediment transport rates and patterns, in addition to coincident tracking of bed composition changes, could provide further insight. Future research questions concern how spatial gradients in sediment transport that cause local erosion or deposition result in changes in bed characteristics, and how those bed characteristics directly alter the transport field through altering the threshold velocity and sediment supply.

Contrary to the spatio-temporal variations in grain size found in the sand scraper measurements, most simulations of coastal sediment transport processes are based on sparse grain size data and commonly assume a homogeneous bed composition within the model domain (Davidson & Turner, 2009; Hallin et al., 2019; Hoonhout & de Vries, 2019; Vousdoukas et al., 2011). Numerical models for coastal applications are typically based on reduced complexity approaches to achieve numerical stability and reasonable simulation times. For most applications, it will not be feasible to incorporate the level of detail on

grain size information that was presented in this study. However, exploratory process-based modeling with variable bed composition could give insights into the errors associated with generalizations of bed composition. Furthermore, a combination of field and model data could be used to explore possible parameterizations of the grain size variability related to marine and aeolian processes.

In the measurements presented in this study, variations in grain size caused by marine processes were often related to morphological change due to bar or berm movement and scarp erosion, matching previous research that showed abundant morphological change in the intertidal zone at the tidal timescale (e.g., Brand et al., 2019; Masselink et al., 2007; Phillips et al., 2019). When erosion occurs, the new vertical variability in grain size is likely partially determined by the exposure of lower-lying sediment layers (Gallagher et al., 2016). Thereby, antecedent sediment deposition can be important for the prediction of sediment availability for aeolian sediment transport. In accretive conditions, synchronization between the transfer of sediment by marine processes and the sediment supply for aeolian sediment transport can occur (Houser, 2009). Coupled numerical models of marine and aeolian processes (e.g., Cohn et al., 2019; Roelvink & Costas, 2019) could be used to quantify the potential influences of horizontal and vertical redistribution of sediments by marine processes on aeolian transport rates.

The effect of marine processes on the grain size distribution can be studied further by collecting additional samples with the sand scraper. These samples can provide the grain size composition that marine processes act upon and consequently the grain composition they leave behind. In this research, measurements were collected at three field sites on only one or several (separate) occasions. However, sampling efforts could be extended in time to investigate the effect of different conditions (varying wave heights, surge heights, etc.) on grain size. For example, Yokokawa and Masuda (1991) showed that variations in deposit thickness were related to the tidal range of a tidal cycle. Thus, samples could be collected throughout a neap-spring cycle to assess the effect of varying tides on changes in grain size distribution. Consequently, these measurements could act as verification for marine process models that show vertical variability in grain size (Reniers et al., 2013; Srisuwan & Work, 2015).

5 | CONCLUSIONS

In this research, a newly developed sand scraper was used to measure the near-surface vertical grain size variability and analyze the effect of marine and aeolian processes on grain size dynamics in the intertidal zone of three different field sites. The sand scraper provides the ability to study the spatial and temporal variations in grain size at a consistent millimeter-scale vertical resolution that was previously not attainable.

The data collectively indicate that there is a cross-shore gradient in grain size across all the measured beaches, reinforcing the concept that beach grain size characteristics are far from homogeneous. Further, alongshore variability, which was prevalent on the mixed-grain, intermediate beach studied here, can dominate over the cross-shore and temporal variability. These insights highlight the limitations of sparse sediment sampling and assumptions that those data are representative for the bed composition over large spatial domains.

The most distinct cases of change in the vertical variability of the grain size distribution by marine processes occurred in cases with significant morphological change during high water. The marine processes resulted both in fining and coarsening of the surface layer. The coarsening was assumed to be related to the formation of a veneer of coarse sediment near the upper limit of wave runup.

During aeolian transport, the expected coarsening of the near-surface grain size was observed in some measurements, however, fining also occurred. The observed sediment fining at the bed surface may be explained by deposition that occurred due to the formation and development of aeolian bedforms within the intertidal zone.

The measurements collected with the sand scraper showed that individual layers can considerately deviate from the vertically averaged median grain size in the upper 50 mm of the bed surface. In addition, the device and data presented in this research can be used to inform future sediment sampling strategies and sediment transport models that investigate the feedbacks between marine and aeolian transport, and the vertical variability of the grain size distribution.

ACKNOWLEDGEMENTS

This work is part of the research programme DuneForce with project number 17064, which is (partly) financed by the Dutch Research Council (NWO). This research could not have been possible without the help of Pieter van der Gaag who designed the Sand Scraper in collaboration with Christa van IJzendoorn and constructed the device together with DEMO (TU Delft). Thanks to DEMO for their close collaboration during the construction and development of the Sand Scraper. We would like to thank the many people that came out to help Christa van IJzendoorn during fieldwork, especially Sander Vos (TU Delft) and Hailey Bond. Thanks to Meagan Wengrove, John Dickey, Peter Ruggiero, and Jeff Wood from Oregon State University for providing support for the field experiment in Waldport, Oregon. Field efforts in Duck, North Carolina, at the U.S. Army Engineer Research and Development Center's (ERDC's) Field Research Facility were executed as part of the During Nearshore Event Experiment (DUNEX), which was facilitated by the U.S. Coastal Research Program (USCRP), and with aeolian transport R&D funding for Nick Cohn through the ERDC Basic Research Program, Program Element 601102/Project AB2/Task 01.

DATA AVAILABILITY STATEMENT

The sand scraper design, the grain size and elevation data, and the software used to analyze the data and create the figures in this publication are available in the 4TU repository, https://doi.org/10.4121/c.5736047.

ORCID

Christa O. van IJzendoorn https://orcid.org/0000-0001-9756-1856
Sierd De Vries https://orcid.org/0000-0001-5865-3715

REFERENCES

Aagaard, T. & Greenwood, B. (2008) Infragravity wave contribution to surf zone sediment transport - the role of advection. *Marine Geology*, 251(1–2), 1–14. Available from: https://doi.org/10.1016/j.margeo.2008.01.017

Anfuso, G. (2005) Sediment-activation depth values for gentle and steep beaches. *Marine Geology*, 220(1–4), 101–112. Available from: https://doi.org/10.1016/J.MARGEO.2005.06.027

Bagnold, R.A. (1937a) The size-grading of sand by wind. *Proceedings of the Royal Society of London. Series a: Mathematical and Physical Sciences*, 163(913), 250–264. Available from: https://doi.org/10.1098/rspa.1937.0225

Bagnold, R.A. (1937b) The transport of sand by wind. *The Geographical Journal*, 89(5), 409. Available from: https://doi.org/10.2307/1786411

Bagnold, R.A. (1941) The physics of blown sand and desert dunes. *The Geographical Journal.*, 98(2), 109. Available from: https://doi.org/10.2307/1787211

Barnard, P.L., Rubin, D.M., Harney, J. & Mustain, N. (2007) Field test comparison of an autocorrelation technique for determining grain size using a digital 'beachball' camera versus traditional methods. *Sedimentary Geology*, 201(1–2), 180–195. Available from: https://doi.org/10.1016/J.SEDGEO.2007.05.016

Bauer, B.O. (1991) Aeolian decoupling of beach sediments. *Annals of the Association of American Geographers*, 81(2), 290–303. Available from: https://doi.org/10.1111/j.1467-8306.1991.tb01691.x

Beven, J. L., Hagen, A. & Berg, R. (2022) Tropical Cyclone Report Hurricane Ida.

Brand, E., De Sloover, L., De Wulf, A., Montreuil, A.L., Vos, S. & Chen, M. (2019) Cross-shore suspended sediment transport in relation to topographic changes in the intertidal zone of a macro-Tidal Beach (Mariakerke, Belgium). *Journal of Marine Science and Engineering*, 7(6), 172. Available from: https://doi.org/10.3390/JMSE7060172

BS1377-2. (1990) Part 2: Classification tests. In: *Methods of tests for soils for civil engineering purposes*. London: British Standard.

Buscombe, D., Rubin, D.M. & Warrick, J.A. (2010) A universal approximation of grain size from images of noncohesive sediment. *Journal of Geophysical Research - Earth Surface*, 115(F2), 2015. Available from: https://doi.org/10.1029/2009JF001477

Çelikoğlu, Y., Yüksel, Y. & Sedat Kabdaşli, M. (2006) Cross-shore sorting on a beach under wave action. *Journal of Coastal Research*, 223(3 [223]), 487–501. Available from: https://doi.org/10.2112/05-0567.1

Chakrabarti, A. (1981) Burrow patterns of Ocypode ceratophthalma (Pallas) and their environmental significance. *Journal of Paleontology*, 55(2), 431–441. Retrieved from https://www.jstor.org/stable/1304229

Clifton, H.E. (1969) Beach lamination: Nature and origin. *Marine Geology*, 7(6), 553–559. Available from: https://doi.org/10.1016/0025-3227(69)90023-1

Cohn, N., Dickhudt, P. & Marshall, J. (2022) In-situ measurement of grain size characteristics within the aeolian saltation layer on a coastal beach. *Earth Surface Processes and Landforms*, 47(9), 2230–2244. Available from: https://doi.org/10.1002/esp.5373

Cohn, N., Hoonhout, B., Goldstein, E., De Vries, S., Moore, L., Durán Vinent, O., et al. (2019) Exploring marine and Aeolian controls on coastal Foredune growth using a coupled numerical model. *Journal of Marine Science and Engineering*, 7(1), 13. Available from: https://doi.org/10.3390/jmse7010013

Davidson, M.A. & Turner, I.L. (2009) A behavioral template beach profile model for predicting seasonal to interannual shoreline evolution. *Journal of Geophysical Research - Earth Surface*, 114(1), F01020. Available from: https://doi.org/10.1029/2007JF000888

Davidson-Arnott, R.G.D., Yang, Y., Ollerhead, J., Hesp, P.A. & Walker, I.J. (2008) The effects of surface moisture on aeolian sediment transport threshold and mass flux on a beach. *Earth Surface Processes and Landforms*, 33(1), 55–74. Available from: https://doi.org/10.1002/esp.1527

de Vries, S., Arens, S.M., de Schipper, M.A. & Ranasinghe, R. (2014) Aeolian sediment transport on a beach with a varying sediment supply. *Aeolian Research*, 15, 235–244. Available from: https://doi.org/10.1016/j.aeolia.2014.08.001

de Vries, S., Verheijen, A., Hoonhout, B., Vos, S., Cohn, N. & Ruggiero, P. (2017) Measured Spatial Variability of Beach Erosion due to Aeolian Processess. *Coastal Dynamics 2017*, (Paper No. 071), 481–491.

Delgado-Fernandez, I. (2010) A review of the application of the fetch effect to modelling sand supply to coastal foredunes. *Aeolian Research*, 2(2–3), 61–70. Available from: https://doi.org/10.1016/j.aeolia.2010.04.001

Doran, K., Long, J. & Overbeck, J. (2015) A method for determining average beach slope and beach slope variability for US sandy coastlines https://doi.org/10.3133/ofr20151053

Edwards, A.C. (2001) Grain size and sorting in modern beach sands. *Journal of Coastal Research*, 17(1), 38–52.

Emery, K.O. (1978) Grain size in laminae of beach sand. *Journal of Sedimentary Research*, 48(4), 1203–1212. Available from: https://doi.org/10.1306/212F7630-2B24-11D7-8648000102C1865D

Field, J.P. & Pelletier, J.D. (2018) Controls on the aerodynamic roughness length and the grain-size dependence of aeolian sediment transport. *Earth Surface Processes and Landforms*, 43(12), 2616–2626. Available from: https://doi.org/10.1002/ESP.4420

Gallagher, E., MacMahan, J., Reniers, A., Brown, J. & Thornton, E. (2011) Grain size variability on a rip-channeled beach. *Marine Geology*, 287(1-4), 43–53. Available from: https://doi.org/10.1016/j.margeo.2011.06.010

Gallagher, E., Wadman, H., McNinch, J., Reniers, A. & Koktas, M. (2016) A conceptual model for spatial grain size variability on the surface of and within beaches. *Journal of Marine Science and Engineering*, 4(2), 38. Available from: https://doi.org/10.3390/JMSE4020038

Gunaratna, T., Suzuki, T. & Yanagishima, S. (2019) Cross-shore grain size and sorting patterns for the bed profile variation at a dissipative beach: Hasaki coast, Japan. *Marine Geology*, 407, 111–120. Available from: https://doi.org/10.1016/J.MARGEO.2018.10.008

Hage, P.M., Ruessink, B.G. & Donker, J.J.A. (2018) Determining sand strip characteristics using Argus video monitoring. *Aeolian Research*, 33, 1–11. Available from: https://doi.org/10.1016/j.aeolia.2018.03.007

Hallin, C., Almström, B., Larson, M. & Hanson, H. (2019) Longshore transport variability of beach face grain size: Implications for dune evolution. *Journal of Coastal Research*, 35(4), 751–764. Available from: https://doi.org/10.2112/JCOASTRES-D-18-00153.1

Hoonhout, B. & de Vries, S. (2017) Field measurements on spatial variations in aeolian sediment availability at the sand motor mega nourishment. *Aeolian Research*, 24, 93–104. Available from: https://doi.org/10.1016/j.aeolia.2016.12.003

Hoonhout, B. & de Vries, S. (2019) Simulating spatiotemporal aeolian sediment supply at a mega nourishment. *Coastal Engineering*, 145, 21–35. Available from: https://doi.org/10.1016/j.coastaleng.2018.12.007

Houser, C. (2009) Synchronization of transport and supply in beach-dune interaction. *Progress in Physical Geography*, 33(6), 733–746. Available from: https://doi.org/10.1177/0309133309350120

Huisman, B.J.A., de Schipper, M.A. & Ruessink, B.G. (2016) Sediment sorting at the sand motor at storm and annual time scales. *Marine Geology*, 381, 209–226. Available from: https://doi.org/10.1016/J.MARGEO.2016.09.005

Jackson, N.L., Masselink, G. & Nordstrom, K.F. (2004) The role of bore collapse and local shear stresses on the spatial distribution of sediment load in the uprush of an intermediate-state beach. *Marine Geology*, 203(1–2), 109–118. Available from: https://doi.org/10.1016/S0025-3227(03)00328-1

Jackson, N.L. & Nordstrom, K.F. (1993) Depth of activation of sediment by plunging breakers on a steep sand beach. *Marine Geology*, 115(1–2), 143–151. Available from: https://doi.org/10.1016/0025-3227(93)90079-B

Kawamura, R. (1951) Study on sand movement by wind. *Rept. Inst. Sci. Technol.*, 5, 95–112.

Larson, M. & Kraus, N.C. (1994) Temporal and spatial scales of beach profile change, duck, North Carolina. *Marine Geology*, 117(1–4), 75–94. Available from: https://doi.org/10.1016/0025-3227(94)90007-8

Lettau, K. & Lettau, H. (Eds). (1978) Experimental and micrometeorological field studies of dune migration. In: *Exploring the World's driest climate*. Madison, WI: Center for Climatic Research, University of Wisconsin-Madison, pp. 110–147.

Masselink, G., Auger, N., Russell, P. & O'Hare, T. (2007) Short-term morphological change and sediment dynamics in the intertidal zone of a macrotidal beach. *Sedimentology*, 54(1), 39–53. Available from: https://doi.org/10.1111/j.1365-3091.2006.00825.x

Masselink, G. & Puleo, J.A. (2006) Swash-zone morphodynamics. *Continental Shelf Research*, 26(5), 661–680. Available from: https://doi.org/10.1016/j.csr.2006.01.015

Medina, R., Losada, M.A., Losada, I.J. & Vidal, C. (1994) Temporal and spatial relationship between sediment grain size and beach profile. *Marine Geology*, 118(3–4), 195–206. Available from: https://doi.org/10.1016/0025-3227(94)90083-3

Nield, J.M., Wiggs, G.F.S. & Squirrell, R.S. (2011) Aeolian sand strip mobility and protodune development on a drying beach: Examining surface moisture and surface roughness patterns measured by terrestrial laser scanning. *Earth Surface Processes and Landforms*, 36(4), 513–522. Available from: https://doi.org/10.1002/esp.2071

O'Dea, A., Brodie, K.L. & Hartzell, P. (2019) Continuous coastal monitoring with an automated terrestrial lidar scanner. *Journal of Marine Science and Engineering*, 7(2), 37. Available from: https://doi.org/10.3390/jmse7020037

Ojeda, E., Ruessink, B.G. & Guillen, J. (2008) Morphodynamic response of a two-barred beach to a shoreface nourishment. *Coastal Engineering*, 55(12), 1185–1196. Available from: https://doi.org/10.1016/J.COASTALENG.2008.05.006

Osborne, P.D. & Rooker, G.A. (1999) Sand re-suspension events in a high energy infragravity swash zone. *Journal of Coastal Research*, 15(1), 74–86.

Phillips, M.S., Blenkinsopp, C.E., Splinter, K.D., Harley, M.D. & Turner, I.L. (2019) Modes of berm and Beachface recovery following storm reset: Observations using a continuously scanning Lidar. *Journal of Geophysical Research - Earth Surface*, 124(3), 720–736. Available from: https://doi.org/10.1029/2018JF004895

Prodger, S., Russell, P. & Davidson, M. (2017) Grain-size distributions on high-energy sandy beaches and their relation to wave dissipation. *Sedimentology*, 64(5), 1289–1302. Available from: https://doi.org/10.1111/sed.12353

Reniers, A.J.H.M., Gallagher, E.L., MacMahan, J.H., Brown, J.A., van Rooijen, A.A., van Thiel de Vries, J.S.M., et al. (2013) Observations and modeling of steep-beach grain-size variability. *Journal of Geophysical Research, Oceans*, 118(2), 577–591. Available from: https://doi.org/10.1029/2012JC008073

Roelvink, D. & Costas, S. (2019) Coupling nearshore and aeolian processes: XBeach and duna process-based models. *Environmental Modelling and Software*, 115, 98–112. Available from: https://doi.org/10.1016/j.envsoft.2019.02.010

Rubin, D.M. (2004) A simple autocorrelation algorithm for determining grain size from digital images of sediment. *Journal of Sedimentary Research*, 74(1), 160–165. Available from: https://doi.org/10.1306/052203740160

Ruggiero, P., Komar, P.D. & Allan, J.C. (2010) Increasing wave heights and extreme value projections: The wave climate of the U.S. Pacific northwest. *Coastal Engineering*, 57(5), 539–552. Available from: https://doi.org/10.1016/J.COASTALENG.2009.12.005

Sallenger, A.H. (1979) Inverse grading and hydraulic equivalence in grain-flow deposits. *Journal of Sedimentary Research*, 49(2), 553–562. Available from: https://doi.org/10.1306/212F7789-2B24-11D7-8648000102C1865D

Schlacher, T.A., Lucrezi, S., Connolly, R.M., Peterson, C.H., Gilby, B.L., Maslo, B., et al. (2016) Human threats to sandy beaches: A meta-analysis of ghost crabs illustrates global anthropogenic impacts. *Estuarine, Coastal and Shelf Science*, 169, 56–73. Available from: https://doi.org/10.1016/J.ECSS.2015.11.025

Sherman, D., Short, A. & Takeda, I. (1993) Sediment mixing-depth and bedform migration in rip channels. *Journal of Coastal Research*, 15, 39–48. Retrieved from https://www.jstor.org/stable/25735722

Sherman, D.J. & Li, B. (2012) Predicting aeolian sand transport rates: A reevaluation of models. *Aeolian Research*, 3(4), 371–378. Available from: https://doi.org/10.1016/j.aeolia.2011.06.002

Sonu, C.J. (1972) Bimodal composition and cyclic characteristics of beach sediment in continuously changing profiles. *SEPM Journal of Sedimentary Research*, 42(4), 852–857. Available from: https://doi.org/10.1306/74d72653-2b21-11d7-8648000102c1865d

Srisuwan, C. & Work, P.A. (2015) Beach profile model with size-selective sediment transport. II: Numerical modeling. *Journal of Waterway, Port, Coastal, and Ocean Engineering*, 141(2), 04014033. Available from: https://doi.org/10.1061/(ASCE)WW.1943-5460.0000274

Stauble, D.K. & Cialone, M.A. (1997) Sediment dynamics and profile interactions: DUCK94. *Proceedings of the Coastal Engineering Conference*, 4, 3921–3934. Available from: https://doi.org/10.1061/9780784402429.303

Strypsteen, G., van Rijn, L.C., Hoogland, M.D., Rauwoens, P., Fordeyn, J., Hijma, M.P., et al. (2021) Reducing aeolian sand transport and beach erosion by using armour layer of coarse materials. *Coastal Engineering*, 166, 378–3839. Available from: https://doi.org/10.1016/J.COASTALENG.2021.103871

Tillotson, K. & Komar, P.D. (1997) The wave climate of the Pacific northwest (Oregon and Washington): A comparison of data sources. *Journal of Coastal Research*, 13(2), 440–452.

Twenhofel, W. H. (1946) Mineralogical and physical composition of the sands of the Oregon coast from Coos Bay to the mouth of the Columbia River.

Uphues, C.F.K., van IJzendoorn, C.O., Hallin, C., Pearson, S.G., van Prooijen, B.C., Miot da Silva, G., et al. (2022) Coastal aeolian sediment transport in an active bed surface layer: Tracer study and conceptual model. *Earth Surface Processes and Landforms*, 47(13), 3147–3162. Available from: https://doi.org/10.1002/ESP.5449

van Bemmelen, C. E. (1988) De korrelgrootte-samenstelling van het strandzand langs de Nederlandse Noordzee-kust - Rijkswaterstaat Rapportendatabank. Retrieved from https://puc.overheid.nl/rijkswaterstaat/doc/PUC_97651_31/

Van der Wal, D. (2000) Grain-size-selective aeolian sand transport on a nourished beach. *Journal of Coastal Research*, 16(3), 896–908.

van der Zanden, J., Hurther, D., Cáceres, I., O'Donoghue, T., Hulscher, S.J. M.H. & Ribberink, J.S. (2017) Bedload and suspended load contributions to breaker bar morphodynamics. *Coastal Engineering*, 129, 74–92. Available from: https://doi.org/10.1016/J.COASTALENG.2017.09.005

Voulgaris, G. & Collins, M.B. (2000) Sediment resuspension on beaches: Response to breaking waves. *Marine Geology*, 167(1–2), 167–187. Available from: https://doi.org/10.1016/S0025-3227(00)00025-6

Vousdoukas, M.I., Almeida, L.P. & Ferreira, Ó. (2011) Modelling storm-induced beach morphological change in a meso-tidal, reflective beach using XBeach. *Journal of Coastal Research*, 64, 1916–1920.

Wiggs, G.F.S., Baird, A.J. & Atherton, R.J. (2004) The dynamic effects of moisture on the entrainment and transport of sand by wind. *Geomorphology*, 59(1-4), 13–30. Available from: https://doi.org/10.1016/j.geomorph.2003.09.002

Yasso, W.E. & Hartman, E.M. (1972) Rapid field technique using spray adhesive to obtain peels of unconsolidated sediment. *Sedimentology*, 19(3–4), 295–298. Available from: https://doi.org/10.1111/j.1365-3091.1972.tb00026.x

Yokokawa, M. & Masuda, F. (1991) Tidal influence on foreshore deposits, Pacific coast of Japan. Clastic Tidal Sedimentology.

Zhenlin Li, M. & Komar, P.D. (1992) Longshore grain sorting and beach placer formation adjacent to the Columbia River. *Journal of Sedimentary Research*, 62(3), 429–441. Available from: https://doi.org/10.1306/D426791A-2B26-11D7-8648000102C1865D

How to cite this article: van IJzendoorn, C.O., Hallin, C., Cohn, N., Reniers, A.J.H.M. & De Vries, S. (2022) Novel sediment sampling method provides new insights into vertical grain size variability due to marine and aeolian beach processes. *Earth Surface Processes and Landforms*, 1–19. Available from: https://doi.org/10.1002/esp.5518